Supplementary Information

Chemoproteomics Reveals Baicalin Activates Hepatic CPT1 to Ameliorate Diet-induced Obesity and Hepatic Steatosis

Jianye Dai[*,†,‡], Kai Liang[‡,§], Shan Zhao[†,‡], Wentong Jia[¶,#], Yuan Liu[*,†,‡], Hongkun Wu[||], Jia Lv[‡,||], Chen Cao[**], Tao Chen[**], Shentian Zhuang[*,†,‡], Xiaomeng Hou[*,†,‡], Shijie Zhou[†,‡], Xiannian Zhang[**], Xiaowei Chen[‡,||], Yanyi Huang[‡,**], Ruiping Xiao[‡,||], Yan-Ling Wang[¶], Tuoping Luo[†,‡], Junyu Xiao[‡,§], Chu Wang[*,†,‡,1]

[*] Synthetic and Functional Biomolecules Center, Peking University, Beijing 100871, China.
[†] Beijing National Laboratory for Molecular Sciences, Key Laboratory of Bioorganic Chemistry and Molecular Engineering of Ministry of Education, College of Chemistry and Molecular Engineering, Peking University, Beijing 100871, China.
[‡] Peking-Tsinghua Center for Life Sciences, Beijing 100871, China.
[§] School of Life Sciences, Peking University, Beijing 100871, China
[¶] State Key Laboratory of Stem Cells and Reproductive Biology, Institute of Zoology, Chinese Academy of Sciences, Beijing, 100101, China.
[#] University of the Chinese Academy of Sciences, Beijing 101408, China.
[||] Institute of Molecular Medicine, Peking University, Beijing, 100871, China.
[**] College of Engineering, Peking University, Beijing 100871, China.

[1]To whom correspondence should be addressed. Email: chuwang@pku.edu.cn

This PDF file includes:

SI Materials and Methods
Figures S1 to S20
Datasets S1 to S3

SI Materials and Methods

Cell culture, modeling, treatment

Hela cells (gifted from Prof. Chengqi Yi's lab from Peking University and authenticated by China Center for Type Culture Collection (Wuhan, China) as free from mycoplasma contamination) were cultured at 37 °C under 5 % CO2 in Dulbecco's modified Eagle's medium (DMEM, Thermo Fisher Scientific) supplemented with 10% fetal bovine serum (Thermo Fisher Scientific), and 1 % penicillin-streptomycin (Thermo Fisher Scientific). 2*104 cells per well were plated in 96-well plates, serum-starved for 24 h and treated with 1 mM free fatty acids (oleic acid : palmitic acid, 2:1,

www.pnas.org/cgi/doi/10.1073/pnas.1801745115

molar ratios, Sigma-Aldrich) for 24 h to induce accumulation of lipid droplets ("modeling") as previously reported.(1) Then the cells were treated with 100 μM baicalin (Sichuan Weikeqi Biological Technology Co., China) or the baicalin BP probe in the high-fat medium for 24 h. For malonyl-CoA treatment, the cells were co-treated with 100 μM malonyl-CoA (Sigma-Aldrich) together with 100 μM baicalin.

RNA interference

The siRNA constructs as listed below were designed and synthesized by GenePharma (Shanghai, China). The interference was performed based on the protocol of Lipofectamine® RNAiMAX (Thermo Fisher Scientific) at the modeling stage before the baicalin treatment.

ALDH3A2_Primer F: CUUUAUGUAUUUUCGCAUAtt
ALDH3A2_Primer R: UAUGCGAAAAUACAUAAAGag
ACSL1_Primer F: GAAGGAUUCUGGUCUGAAAtt
ACSL 1_Primer R: UUUCAGACCAGAAUCCUUCcc
ACSL 3_Primer F: GGAACUAACUGAACUAGCUtt
ACSL 3_Primer R: AGCUAGUUCAGUUAGUUCCtt
ACSL 4_Primer F: GCAAUAAUCCUGCUAUGGAtt
ACSL 4_Primer R: UCCAUAGCAGGAUUAUUGCag
CPT1A_Primer F: GGAUGGGUAUGGUCAAGAUtt
CPT1A_Primer R: AUCUUGACCAUACCCAUCCag
ACADVL_Primer F: GAUUGUCAAUGAACAGUUUtt
ACADVL_Primer R: AAACUGUUCAUUGACAAUCcc
HADHA_Primer F: CCGUCCUUAUCUCAUCAAAtt
HADHA_Primer R: UUUGAUGAGAUAAGGACGGca

CPT1A overexpression in hela cell

The overexpression constructs were listed on “Cloning of CPT1 expression plasmids” as followed. The overexpression was performed based on the protocol of Lipofectamine® 3000 (Thermo Fisher Scientific) at the modeling stage before the baicalin treatment.

<u>qRT-PCR</u>

Total RNAs were extracted following the instructions of Eastep Super Total RNA Extraction (LS1040, Promega). The reverse transcription were adapted from protocols of RevertAid First Strand cDNA Synthesis Kit (#cat: K1622, Thermo Fisher Scientific). qRT-PCR samples were prepared as the protocol of UltraSYBR Mixture(With ROX I)(#cat: CW2601, cwbiotech) with the primers designed and synthesized by TSINGKE (Beijing, China). The samples were analyzed on Applied Biosystems ViiA 7 systems (Thermo Fisher Scientific) were used for qRT-PCR analysis.

ALDH3A2_Primer F: ACTGATAGGAGCCATCGCTGCA
ALDH3A2_Primer R: GCTCCGTGGTTTCCTCAACACC
ACSL1_Primer F: ATCAGGCTGCTCATGGATGACC
ACSL 1_Primer R: AGTCCAAGAGCCATCGCTTCAG
ACSL 3_Primer F: CTTTCTCACGGATGCCGCATTG
ACSL 3_Primer R: CTGCTGCCATCAGTGTTGGTTTC
ACSL 4_Primer F: GCTATCTCCTCAGACACACCGA

ACSL 4_Primer R: AGGTGCTCCAACTCTGCCAGTA
CPT1A_Primer F: GATCCTGGACAATACCTCGGAG
CPT1A_Primer R: CTCCACAGCATCAAGAGACTGC
ACADVL_Primer F: TAGGAGAGGCAGGCAAACAGCT
ACADVL_Primer R: CACAGTGGCAAACTGCTCCAGA
HADHA_Primer F: GCCGACATGGTGATTGAAGCTG
HADHA_Primer R: GGAGAGCAGATGTGTTACTGGC

Transcriptome analysis by RNA-seq

Total RNAs were extracted following the instructions of RNeasy Micro Kit (#cat: 74004, QIAGEN). The mRNA isolation and cDNA synthesis were adapted from protocols in NEBNext Ultra RNA Library Prep Kit for Illumina (E7530, New England Biolabs). 50 ng cDNA of each sample were used as the start amount of libraries preparation. The pair-end sequencing libraries with ~300 bp insert size were constructed following the instructions of NEBNext Ultra DNA Library Prep Kit for Illumina (E7370, New England BiolabsA). Illumina HiSeq 2500 systems were used for sequencing. Fragments per kilobase of exon model per million mapped reads (FKPM) of every mRNA were used for further analysis.

MTT assay

104 cells were plated in 96-well plates with 100 μL of pre-warmed medium per well. After adherence, cells were starved in serum-free medium for 24 h and then switched to regular medium containing 100 μM of baicalin or the baicalin BP probe for another 24 h. After the treatment, the cells were incubated with 100 μL of regular medium with 50 μg MTT (Sigma-Aldrich) for 4 h. Finally, the purple precipitates were dissolved in 200 μL of DMSO (Sigma-Aldrich) for measurement of absorbance at 490 nm by a microplate reader (Bio-Rad).

Oil Red O (ORO) staining and quantitation assay

Cells were washed with PBS buffer 3 times and fixed in ice-cold 10 % formalin for 30 mins. The fixed cells were stained in 100 μL of 0.5 % Oil Red O in isopropanol/water solution (3:2, v/v, Sigma-Aldrich) for 20 mins, differentiated in 75 % ethanol for 2 mins and finally rinsed with 100 μL of distilled water 3 times before imaging. Intensities of each image was analyzed with ImageJ and normalized by the cell count. For quantitation of cellular lipids, 50 μL of DMSO (Sigma-Aldrich) were added to dissolve the ORO dyes extracted from the stained cells and the absorbance at 490 nm measured by a microplate reader (Bio-Rad) were normalized by the MTT measurements to yield a final quantitative readout.

Stimulated Raman Scattering (SRS) Microscopy

The SRS microscopy used to determine lipid content was performed on an in-house built system as previously reported(2). Cells were treated with 1mM free fatty acids for 24h followed by co-treatment with 100 μM baicalin for another 24 h in 35 mm petri dishes with glass bottom, and scanned with the SRS system. To probe the lipid content, pump and probe frequency difference was tuned to 2850 cm-1, which is in resonance with the CH2 symmetric vibration mode in live cells. Three random field of views were selected for imaging. 3-dimensional images were acquired in each field of view to get

complete lipid distribution. 10-15 mins were taken for each dish. The intensity of each image was analyzed with ImageJ and normalized by the cell count.

Synthesis of the baicalin probes

The route for synthesizing the baicalin probes is shown in Fig. S3.

To a solution of 1 (1.0 g, 6.22 mmol) in DMF (12 mL) was added NaN3 (606 mg, 9.33 mmol) and NH4Cl (333 mg, 6.22 mmol). The reaction mixture was heated to 120 °C and was stirred overnight. The reaction mixture was then quenched with Na2CO3 and acidized with 2 M HCl to obtain precipitates, which was collected by filtering to give product 2 (1.3 g, 98 % yield). To a solution of 2 (304 mg, 1.49 mmol) in DMSO (12 mL) was added (4-hydroxyphenyl) boronic acid (411 mg, 2.98 mmol) and Cu2O (11 mg, 0.075 mmol). The reaction mixture was heated to 100 °C and was stirred overnight. The reaction mixture was extracted with EA and washed with 2 M HCl and saturated NaCl solution. The organic solution was evaporated in vacuo. The residue was purified by flash chromatography on silica gel to give compound 3 (188 mg, 42 % yield).

Under a nitrogen atmosphere, to a dry DMF solution (6 mL) of 3 (180 mg, 0.61 mmol) at 0 °C were added NaH (18 mg, 0.73 mmol) and 3-bromoprop-1-yne (81 μL, 0.730 mmol) slowly. After raising the reaction temperature to room temperature gradually, the solution was stirred overnight. The reaction mixture was quenched with saturated ammonium chloride, extracted with EA and dried over sodium sulfate. Then the organic solvent was removed under vacuum, and the residue was purified by flash column chromatography on silica gel using PE/EA as the eluent to give product 4 (175 mg, 86 % yield).

Compound 4 (149 mg, 0.45 mmol) was dissolved in a mixture solution of THF/MeOH/H2O (8/2.5/2.5 mL). Then LiOH (94 mg, 2.23 mmol) was added. The reaction mixture was reflux at 65 °C for 2 h. The reaction mixture was acidized with 2 M HCl to obtain precipitates, which was collected by filtering to give the acid product. To the EA (18 mL) solution of the crude acid from the previous step was added (4-(aminomethyl)phenyl)(phenyl)methanone (5, 122 mg, 0.49 mmol), EDCI (94 mg, 0.49 mmol) and HOAt (67 mg, 0.49 mmol). The reaction mixture was stirred for 4 h at RT, then washed with saturated NaHCO3 and brine. The organic solvent was removed under vacuum, and the residue was purified by flash column chromatography on silica gel using PE/EA as the eluent to give product 6 (126 mg, 55 % yield over two steps).

The solution (DMSO/EtOH/H2O solvent) of Baicalin (22 mg, 0.049 mmol) and 6 (25 mg, 0.049 mmol) within a quartz test tubes was irradiated for 3 h using a hand-held 302 nm UV lamp under stirring. The organic solvents were evaporated under reduced pressure. The product 7 were purified by HPLC-MS (25.2 mg, 55 % yield). 1H NMR (500 MHz, MeOD) δ 8.07 (m, 2H), 7.94-7.89 (m, 3H), 7.83-7.81 (d, J = 7.82, 1H), 7.74-7.72 (d, J = 7.73, 4H), 7.64-7.42 (m, 10H), 7.09-6.75 (m, 4H), 4.72-4.61 (m, 4H), 4.07-3.88 (m, 2H), 3.66-3.58 (m, 2H), 3.44-3.40 (t, J =3.42, 1H), 2.92-2.91 (m, 1H); 13C NMR (500 MHz, MeOD) δ 196.83, 183.17, 167.74, 167.25, 166.04, 165.22, 158.13, 150.98, 149.83, 147.09, 143.91, 137.49, 136.28, 134.78, 134.57, 134.09, 132.36, 131.83, 131.44, 130.00, 129.55, 129.16, 129.01, 128.75, 128.10, 127.58, 127.31, 127.27, 127.13, 127.08, 126.77, 126.40, 115.36, 114.81, 106.82, 104.78, 101.54, 95.54,

77.78, 75.96, 75.55, 75.20, 72.89, 72.47, 71.04, 55.44, 42.95, 39.03; HRMS-EI (m/z) calc. for C52H42N3O14 [M+]: 932.2715; Found: 932.2713.

In-gel fluorescence analysis

Hela cells were serum-starved for 24 h and treated with 1 mM free fatty acids for 24 h to induce accumulation of lipid droplets. The cells were harvested and stored at -80 °C for further experiments.

Frozen cell pellets were re-suspended in PBS with 0.1% Triton X-100 (Sigma-Aldrich) on ice, sonicated and separated into soluble and insoluble fractions by ultracentrifugation at 20,000 g for 30 mins. The concentration of soluble lysates was determined using the BCA protein assay (Pierce™ BCA Protein Assay Kit, Thermo Fisher Scientific) on a microplate reader (Bio-Rad) and adjusted to 2 mg/mL. The lysate (200 μL per aliquot) was labeled with the baicalin probe (200 μM) with or without competition of the native compound (400 μM). The probe-labeled lysates were precipitated with chloroform-methanol, re-suspended with 200 μL of 1.2% SDS/ PBS and mixed with 300 μM rhodamine-azide, 1 mM Tris(2-carboxyethyl)phosphine (TCEP, Sigma-Aldrich), 100 μM Tris((1-benzyl-1H-1,2,3-triazol-4-yl)methyl)amine (TBTA) (Sigma-Aldrich), and 1 mM CuSO4 (Sigma-Aldrich) at room temperature. After 1 h, samples were mixed with SDS sample loading buffer and separated by 10% SDS-PAGE. The image of rhodamine fluorescence was acquired on a Biorad ChemiDoc imaging system and was shown in Fig. S3.

CPT1 activity assay

The CPT1 activity assay was performed according to a modified protocol reported previously(3), which basically measures the conversion of deuterium-labeled carnitine ([D9]-carnitine, Cambridge Isotope Laboratory) to deuterium-labeled palmitoyl-carnitine ([D9]-palmitoyl-carnitine). The reaction buffer is composed of 150 mM KCl (Sigma-Aldrich), 2 mM EDTA (Sigma-Aldrich), 4.5 mM glutathione (Sigma-Aldrich), 1 mg/mL BSA, 0.1 mM palmitoyl-CoA (Sigma-Aldrich) and 0.1 mM [D9]-carnitine in PBS. Baicalin was added as indicated concentrations. We used the pure but inactive recombinant CPT1A to establish a protein concentration standard curve and use western blot to estimate the amount of CPT1A in various cell, tissue and E.coli lysates when we performed the CPT1A enzymatic assay. These numbers were then used to normalize CPT1A activity to an absolute scale (conversion of nmol of palmitoyl-carnitine per min per ❣ g of CPT1A)

To test cellular CPT1A activity, HeLa cells were lysed in PBS with 0.1% of Triton X-100 (Sigma-Aldrich) on ice, and the lysates were adjusted to 2 mg/mL. The enzymatic reaction was started by adding 20 μL of lysates to 100 μL of the reaction buffer and incubated at 37 °C for 10 mins. At the end of reaction, 0.3 nmol of [D3]-palmitoyl-carnitine (Cambridge Isotope Laboratory) was added as internal standard and 600 μL of precooled methanol was added to extract the small-molecule metabolites on ice. The reaction mixture was centrifuged at 20,000 g for 5 mins at 4 °C. Then 400 μL of the supernatant were taken out and mixed with 600 μL of distilled water to make 1 mL of the final sample volume for measurement of [D9]-palmitoyl-carnitine by LC-MS. The LC-MS system is composed of an AB SCIEX 5500 triple-quadrupole mass spectrometer and a SHIMADZU DGU-20A liquid chromatography instrument with an

Agilent column. The buffer gradient is 100%-0 Buffer A (100% water, 0.1% formic acid) and 0%-100% Buffer B (100% acetonitrile, 0.1% formic acid) for 10 mins. The absolute concentration of [D9]-palmitoyl-carnitine is calculated by comparing the peak areas of [D9]-palmitoyl-carnitine and [D3]-palmitoyl-carnitine. Two reactions were prepared in parallel with or without 100 μM of malonyl-CoA treatment and the activity of CPT1A was calculated as the difference in [D9]-palmitoyl-carnitine between with and without malonyl-CoA treatment.

To test CPT1A activity in primary hepatocytes, hepatocytes were lysed in PBS with 0.1% of Triton X-100 (Sigma-Aldrich) on ice, and the lysates were adjusted to 2 mg/mL. The enzymatic reaction was started by adding 10 μL of lysates to 100 μL of the reaction buffer and incubated at 37 °C for 10 mins.

To test CPT1A activity from mitochondria, the mitochondria were isolated by Mitochondria Isolation Kit for Cultured Cells (Thermo Fisher Scientific). Then the mitochondria were lysed in PBS with 0.1% of Triton X-100 (Sigma-Aldrich) on ice, and then the lysates were adjusted to 0.2 mg/mL. 10 μL of mitochondrial lysates were used to assay CPT1A activity as described above.

To test CPT1A activity from mouse livers, the tissues were homogenized with 0.1 % of Triton X-100 to obtain the lysates at 2 mg/mL. 10 μL of liver lysates were used to assay CPT1A activity as described above.

To test recombinant CPT1 activity from E. coli, 10 μL of lysates (1L E. coli cultures lysed by 50mL PBS with 0.1% triton-100) of E. coli overexpressing each CPT1 construct were used to assay CPT1 activity as described above except that the measurement of [D9]-palmitoyl-carnitine was performed without malonyl-CoA treatment as the control in calculating the CPT1 activity.

SILAC-ABPP

The SILAC ABPP experiments were performed based on protocols adapted from previous reports(4)-(5). Hela cells were passaged 10 times in SILAC DMEM (Thermo Fisher Scientific) with 10 % SILAC FBS (Thermo Fisher Scientific), 1 % penicillin-streptomycin (Thermo Fisher Scientific), and 100 μg/mL [13C6,15N4]L-arginine-HCl and [13C6,15N2]L-lysine-HCl (Cambridge Isotope Laboratory) or L-arginine-HCl and L-lysine-HCl (Sigma-Aldrich). Before ABPP experiment, cells were serum-starved for 24 h and treated with 1 mM free fatty acids for 24 h to induce accumulation of lipid droplets. The cells were harvested and stored at -80 °C for further experiments.

Frozen cell pellets were re-suspended in PBS with 0.1% Triton X-100 (Sigma-Aldrich), sonicated and separated into soluble and insoluble fractions by ultracentrifugation at 100,000 g for 45 min. The soluble protein concentration was determined using the BCA protein assay (Pierce™ BCA Protein Assay Kit, Thermo Fisher Scientific) on a microplate reader (Bio-Rad). The lysates were adjusted to 2 mg/mL and treated with 2 mM baicalin (10 μL of 200 mM stock in DMSO) or DMSO, labeled with 200 μM of the baicalin probe (10 μL of 20 mM stock in DMSO) or DMSO, and then put on ice under UV radiation at 365 nm for 1 h. The light and heavy probe-labeled proteome were mixed equally in a 1:1 ratio and immediately precipitated with chloroform-methanol. Then the precipitations were re-suspended with 1.2 % SDS/ PBS and combined with 300 μM biotin-azide, 100 μM TBTA, 1 mM TCEP, and 1 mM

CuSO4 for 1 h. After this reaction, the proteomes were extracted again with chloroform-methanol to remove redundant reagents. The protein interphase was washed with cold methanol, solubilized with 1.2 % SDS/ PBS and diluted 5x with PBS. The solubilized proteins were incubated with streptavidin beads (100 μL of slurry, Thermo Fisher Scientific) at room temperature for 3 h with rotation. The beads were then washed with 5 mL of PBS three times and 5 mL of water three times before being transferred to a screw-top Eppendorf tube. The enriched proteins were denatured in 6 M urea/PBS, reduced with 10 mM dithiothreitol (DTT, J&K Scientific) at 65 °C for 15 mins and blocked with 20 mM iodoacetamide (Sigma-Aldrich) at 35 °C for 30mins in dark with agitation. The reaction was diluted with 950 μL of PBS and centrifuged at 1400 g for 3 mins. The supernatant was removed. Then the beads were added with a premixed solution of 200 μL of 2 M urea/PBS, 2 μL of 100 mM calcium chloride in water and 4 μL of trypsin (20 μg reconstituted in 40 μL of the trypsin buffer, Promega) and incubated at 37 °C with agitation overnight. Next day the mixture was transferred to a Bio-spin filter (Bio-Rad) and the digested solution was eluted into a low-adhesion tube by centrifugation (1000 g). The eluents were acidified with 5% formic acid.

As illustrated in Fig. 2c, a series of SILAC-ABPP experiments using the baicalin probe with or without competition of the native baicalin compound were performed. Briefly, light proteomes were always treated with DMSO and labeled by the baicalin BP probe via UV-induced photo-crosslinking and then mixed with the heavy proteomes processed as described below. In the "BP control" experiment, heavy proteomes were treated with DMSO and labeled with a blank DMSO solution with UV radiation. In the "UV control" experiment, heavy proteomes were treated with DMSO and labeled with the baicalin BP probe but without UV radiation. In the "CP control" experiment, heavy proteomes were treated with DMSO and labeled with the baicalin CP probe (i.e., without the benzophenone moiety) with UV radiation. In the "competition" experiment, heavy proteomes were competed with baicalin and labeled by the baicalin BP probe with UV radiation. The three control experiments were designed to eliminate false positive targets from indirect and/or non-specific binding to the probe. Three replicates were performed for each control and competition experiment and all the proteins quantified were listed in Dataset S1.

Competitive ABPP-RD

100 μL of E. coli lysates with recombinant CPT1A (3 mg/mL in 100 mM TEAB buffer) were incubated with baicalin or DMSO respectively, and photo-labeled with 200 μM of the baicalin BP probe. The labeled proteomes were extracted with chloroform-methanol, washed with cold methanol, and then solubilized with 100 μL of 1.2% SDS/TEAB. 10 μL of the probe-labeled lysates were mixed with 30 μL of 8 M Urea/TEAB, reduced by 10 mM DTT (J&K Scientific) at 65 °C for 15 mins and blocked with 20mM iodoacetamide (Sigma-Aldrich) at 35 °C for 30 mins in dark. The reaction mixture was diluted to 2M Urea/TEAB and digested with 0.4 μg of trypsin overnight at 37 °C with agitation. The digested samples were desalted with C18 spin columns (Thermo Fisher Scientific) and dried by vacuum centrifugation (1500 rpm, room temperature). The dried samples were reconstituted in 100 μL of 100 mM TEAB and subjected to the reductive dimethylation as previously reported (6). Briefly, 8 μL of 4 %

(v/v) CH2O or 13CD2O (Sigma-Aldrich) were added to the DMSO-treated and baicalin-treated samples, respectively, and reduced with 8 μL of 0.6M NaBH3CN for 1 h at room temperature. The reaction was quenched with 32 μL of 1 % (v/v) ammonia solution and 16 μL of formic acid. The pair of light and heavy samples were combined, desalted and dried by vacuum centrifugation. Finally, the dried samples were reconstituted in 20 μL of Buffer A (95 % water, 5 % acetonitrile, 0.1 % formic acid) for LC-MS/MS analysis.

LC-MS/MS analysis

The LC-MS/MS analysis were performed on a Q-Exactive Orbitrap mass spectrometer (Thermo Fisher Scientific) coupled with an Ultimate 3000 LC system using a published protocol(5). Briefly, the flow rate through the column was set to 0.3 μL/min and the applied distal spray voltage was set to 2.8 kV. MS2 data collection was performed using one full scan (350–1,800 MW) followed by data-dependent MS2 scans of the most 20 abundant ions with dynamic exclusion enabled.

MS data analysis

Peptide search was performed using ProLuCID(7) with variable modification of methionine (15.9949 Da), static modification of cysteine (57.0215 Da) and full trypsin specificity. The data was further filtered by DTASelect 2.0.47 (8) with a false discovery rate of 1 %.

SILAC-ABPP ratios were quantified using an in-house software CIMAGE as described before(9) with slight modifications. The peptide with chromatographic peak detected in only the light sample but not the heavy one was assigned with a threshold ratio of 15 to reflect the specific enrichment. Only proteins that were quantified in all three replicates with an averaged SILAC ratio (light/heavy) above 4.0 were selected for further GO analysis.

For competitive ABPP-RD, the isotopic dimethylations (28.0313 and 34.0631 Da for light and heavy labeling, respectively) were set as variable modifications on the N-terminal of a peptide and lysines. The quantitation was done by CIMAGE accordingly.

Cloning of CPT1 expression plasmids

There are two isoforms for human CPT1A with the isoform 1 from residue 1 to 773, and the isoform 2 from residue 1 to 756. The difference between the isoform1 and isoform 2 starts from residue 746 to the C terminal. In order to clone the longer isoform 1, we first cloned the sequence of isoform 2 from its cDNA and combined with a synthesized nucleotide sequence 2236-2319 of the isoform1 by using bridge PCR. We then cloned the full sequence of the isoform 1 into the pQLinkMx vector between EcoR 1 and Not 1 sites to obtain the expression plasmid.

Primers for bridge PCR were as follows:

Primer F CCGGAATTCATGGCAGAAGCTCACCAAGC;

Primer R’ CAAAGCGATGAGAATCCGTCTCAGGGCAAGAG;

Primer F’ CTCTTGCCCTGAGACGGATTCTCATCGCTTTG;

Primer R ATAAGAATGCGGCCGCTTACTTTTTGGAATTAGAACTGAGACC.

Each of the full length DNA sequences of human CPT1B (hCPT1B), human CPT1C (hCPT1C) or C.elegans CPT1 (ceCPT1) was cloned into a pQLinkMx vector between the Sac 1 and Not 1 sites. The full length DNA sequence of Mus musculus

CPT1A (mCPT1A) was cloned between the EcoR 1 and Not 1 sites. Primers were as listed as follows:
hCPT1B_Primer F: CGAGCTCATGGCGGAAGCTCACCAG;
hCPT1B_Primer R: ATAAGAATGCGGCCGCTCAGCTGTAGGCCTTGGGAAC.
hCPT1C_Primer F: CGAGCTCATGGCTGAAGCGCACCAG;
hCPT1C_Primer R: ATAAGAATGCGGCCGCTCAGAAGTCGGTGGATGTCATTG.
ceCPT1_Primer F: ACGCGTCGACAAATGGCTGAGGCACGCAGTG
ceCPT1_Primer R: ATAAGAATGCGGCCGCTTATTGCTTTTTCTTCGGCGC
mCPT1A_Primer F: CCGGAATTCATGGCAGAGGCTCACCAAG
mCPT1A_Primer R: ATAAGAATGCGGCCGCTTACTTTTTGGAATTGGCGGTG

Mutants of human CPT1s were generated by PCR according to Site Directed Mutagenesis Protocol (10). All constructs were checked by DNA sequencing.

Primers for disruptive mutants of hCPT1A were listed as follows:
hCPT1A_L286W_Primer F: CCTGCTTTACAGGCGCAAATTGGACCGGGA;
hCPT1A_L286W_Primer R: ATTTGCGCCTGTAAAGCAGGATGGCATGG.
hCPT1A_I291F_Primer F: GCAAACTGGACCGGGAGGAATTCAAACCAAT;
hCPT1A_I291F_Primer R: ATTCCTCCCGGTCCAGTTTGCGCCTGTAAAG.
hCPT1A_E309Y_Primer F: CACTCTGCTCCGCTCAGTGGTACCGGATGTTT;
hCPT1A_E309Y_Primer R: GTACCACTGAGCGGAGCAGAGTGGAATCGT.
hCPT1A_H327E_Primer F: GAGACAGACACCATCCAGGAAATGAGAGAC;
hCPT1A_H327E_Primer R: TTCCTGGATGGTGTCTGTCTCCTCTCCTGG.

Primers for active site mutants of human CPT1A were as follows:
hCPT1A_H473A_Primer F: GCTCAACGCTGAAGCCTCCTGGGCAGATGCG
hCPT1A_H473A_Primer R: GGCTTCAGCGTTGAGGCCCATCTTCCCG

Primers for wildtype and disruptive mutants of Mus musculus CPT1A (mCPT1A) for animal experiments were as follows with all constructs checked by DNA sequencing:
mCPT1A_PrimerF: CGGGATCCATG GCAGAGGCTCACCAA
mCPT1A_PrimerR: CCGCTCGAGTTACTTTTTGGAATTGGCGG
mCPT1A_H327E_PrimerF:GACAGACACCATCCAAGAGGTCAAGGACAGCAG
G
mCPT1A_H327E_PrimerR: CCTGCTGTCCTTGACCTCTTGGATGGTGTCTGTC

We also made constructs of hCPT1A for overexpression in Hela cells. Sequence of wild-type hCPT1A was cloned into a pCLHCY vector. Each of the disruptive mutations were generated in the same way as described above, including L286W, I291F, E309Y and H327E. All constructs were verified by sequencing.

Recombinant expression of CPT1 in E. coli

Expression plasmids were first transformed into E.coli BL21. Cells were grown (1L medium in 3L bottle) at 37 °C to an absorbance of 0.8-1.0 at 600 nm and induced by 0.5 mM IPTG for 20 h. Cells were lysed by high pressure homogenization at 800 bar for 3 mins in PBS buffer with 0.1 % Triton X-100 (Sigma-Aldrich) and 1 mM PSMF (AMRESCO). The mixture was centrifuged at 21,500 rpm for 1 h. The abundance of CPT1 in both pellet and supernatant were analyzed by 10% SDS-PAGE.

Animal works

All animal procedures were performed in accordance with protocols approved by the Committee for Animal Research of Peking University, China, and conformed to the Guide for the Care and Use of Laboratory Animals (NIH publication No. 86-23, revised 1985). All mice (C57BL/6j, Charles River, Beijing, China) were maintained in a temperature-controlled barrier facility with a 12-h light/dark cycle and were given free access to food and water in the Center for Experimental Animals at Peking University, Beijing, China (an AAALAC-accredited experimental animal facility). Only male animals were used in this study. The study was stratified randomized block according to the weight. Five mice per group were chosen to reach statistical significance. The research used the random, contrast and single-blinded test. Dietary interventions with a high-fat diet (60 % calories from fat, Research Diets Inc.) or a chow diet (10% calories from fat, Research Diets Inc.) were started at the age of 6 weeks for wild-type littermates and maintained for 24 weeks(11). The daily intragastric administrations of 400 mg/kg baicalin (40 mg/mL saline stock) (12) were started after 12-week dietary intervention and maintained for another 12 weeks before these mice were analyzed for metabolic changes and steatosis-related symptoms.

Liver-specific knockdown of CPT1A

Lentiviral vector construction and virus production were generated as described previously(13). We initially performed the screening of shRNAs targeting CPT1A entire genomes using BLOCK-iT™ RNAi Designer (http://rnaidesigner.invitrogen.Com /rnaiexpress/). According to the start position and rank, we selected the target sequences (GGAGACAGACACCATCCAACA) to construct a lentiviral shRNA, and the XhoI and HpaI restriction sites following U6 promoter were used to insert shRNA into the third generation lenti backbone pLL3.7 (#cat: 11795, Addgene) . The positive purified lentiviral shRNA-expressing plasmid or an empty plasmid (as negative control) were transfected with the packaging plasmids (pMDLg/pRRE, CMV-VSVG and RSV-Rev) into HEK 293T cells for lentivirus production, respectively. After 48 h transfection, the viral supernatants were harvested, ultra-centrifuged, re-suspended in PBS and stored at -80 °C until use. The virus titers, determined by infecting HEK 293T cells with serial dilutions of concentrated lentivirus, were approximately $6*10^8$ IFU/mL. The viruses were injected to animals through tail vein once every four weeks.

Liver-specific overexpression of CPT1A

The Adeno-associated virus (AAV) delivery system was used for overexpression of Cpt1a (AAV2/8-Tbg-Cpt1a) and Cpt1a H327E (AAV2/8-Tbg-Cpt1a H327E) in mice liver, with the AAV2/8-Tbg-GFP served as a control. The target sequences of Cpt1a and Cpt1a H327E were inserted between the NotI and BamHI restriction sites following Tbg promoter into AAV backbone, respectively. The AAV2/8 vector was generated by transfecting three plasmids (pAAV containing Cpt1a or Cpt1a H327E, pAAV2/8-trans plasmid and helper plasmid) in HEK 293T cells. Titers of the vector genome were measured by qPCR with vector-specific primers. The mice were injected with 100 μL of virus containing 10^{11} AAV2/8 vector genomes via the tail vein.

Primary hepatocyte isolation and culture.

Primary hepatocytes were isolated from the livers of 6-8 weeks male mice using the collagenase perfusion method. Briefly, after the tissues were digested by a perfusion of collagenase type IV solution (#cat: 17104019, Invitrogen), the liver was dissected, minced and filtered through a 70μm cell strainer (#cat: 352350, Falcon). The mixture was centrifuged at 50g to collect hepatocytes (the pellet). The resuspended hepatocytes were seeded on plates in DMEM with 10% FBS and 1% penicillin–streptomycin (PS).

Histological analysis

Liver samples, dissected from the same lobe of each animal, were fixed in 4% paraformaldehyde overnight at room temperature, dehydrated through ethanol gradients, infiltrated in xylene and embedded in paraffin. Serial sections of 5 μm thickness were made from paraffin embedded tissue for hematoxylin and eosin (H&E) staining. Another set of liver samples, taken from the same lobe of each animal, were snap-frozen in liquid N2 and stored at -80 °C. The frozen samples were embedded in Tissue-Tek® O.C.T. and cryosectioned (10 μm thick) for Oil Red O staining.

Biochemistry indexes and metabolic rate measurements

Serum AST, ALT, TG, CHOL, LDL, HDL, APOE, TNTs and GLU were measured by automatic biochemical analyzer (Roche, Cobas 4000). For liver triglyceride and cholesterol measurement, tissue extracts were prepared by homogenizing 0.2 g of raw liver tissues in chloroform: methanol (2:1, v/v) (14).

For GTTs, mice were fasted overnight for 16 h and then injected intraperitoneally (i.p.) with D-glucose (2 g/kg body weight). For ITTs, mice were fed and i.p. injected with bovine insulin (0.75 U/kg body weight, Sigma-Aldrich). Blood samples were collected from the tail vein before and after injection. Glucose concentrations were measured with an AccuCheck blood glucose meter (Roche). (15)

To measure food intake, ambulatory activity and other metabolic parameters(15), mice were housed individually under a 12-h light/ dark cycle. A comprehensive animal metabolic monitoring system (CLAMS; Columbus Instruments) was used to evaluate oxygen consumption (VO_2) and carbon dioxide production (VCO_2) continuously. Energy expenditure was calculated using the formula: energy expenditure = $(3.815+1.232VO_2/VCO_2)/VO_2$; respiratory exchange ratio (RER) = VCO_2/VO_2

Computational modelling

The homology model of CPT1A (excluding residues 1-149 in the N-terminal transmembrane domain) was automatically built on the Robetta structure prediction sever(16). Potential binding pockets inside the protein were predicted using the fpocket program(17). Using the information obtained from the competitive ABPP-RD experiments as constraints, we pre-docked baicalin into a binding pocket in CPT1A using Autodock Vina program(18). To introduce backbone flexibility, we further optimized the docking model using the Rosetta ligand docking protocol (19). In order to validate the model, four "disruptive" mutations were obtained by using the single-site saturation mutagenesis scanning protocol in Rosetta(20) based on the following two criteria: each of the mutants should 1) maintain similar structural stability to the wild type protein (energy difference < 3.0 Rosetta Energy Units (REU)) and 2) destabilize the interaction between CPT1A and baicalin (energy increase > 3.0 REU). The Rosetta energy scores for these four mutants can be found in Fig. S10

Western blot

The antibody for CPT1A was purchased from Abcam (#cat: ab128568), and beta-actin was purchased from TransGen Biotech (#cat: HC201-02). Tissues or cells were lysed in PBS buffer with 0.1% Triton X-100 on ice for 30 min. After short pulses of sonication, the lysates were centrifuged and adjusted to 1 mg/mL. 15 μg of the lysates were separated by 10 % SDS-PAGE gel and immunoblotted for CPT1A.

Thermal shift assay

The thermal shift assay was performed as previously described(21)-(22). For the temperature-dependent thermal shift assay, 50 μL of lysates (3 mg/mL) from steatosis Hela cells or CPT1A-overexpressing *E.coli* were incubated with 100 μM of baicalin at each temperature point from 36 to 76 °C for 4 min. The samples were centrifuged at 20,000 g for 10 mins at 4 °C to separate the supernatant and pallet. 12 μL of the supernatant was mixed with 3 μL of 5x loading buffer and then separated on a 10 % SDS-PAGE for immunoblotting analysis of CPT1A.

For the dose-dependent thermal shift assay, 50 μL of lysates (3 mg/mL) were incubated with various concentrations of baicalin (between 0 to 1000 μM) at 52 °C for 4 min. The supernatant was isolated by centrifugation and subjected to immunoblotting analysis of CPT1A as described above.

Statistics

Statistical Product and Service Solutions (IBM SPSS) was used to test the data normality and homogeneity of variance by Kolmogorov-Smirnov test and Levene's test respectively. When three or more means are compared for statistical significance, one- or two-way ANOVA was conducted with treatment or phenotype as the independent factors. When two groups of measurements were examined for statistical significance, the two-sided Student's t-test was conducted. P-values <0.05 are considered statistically significant. Unless otherwise specified, all data are presented as mean ± s.e.m.

Data Availability

All the data that support the findings of this study including mass spectrometry data are freely available from the corresponding authors upon request.

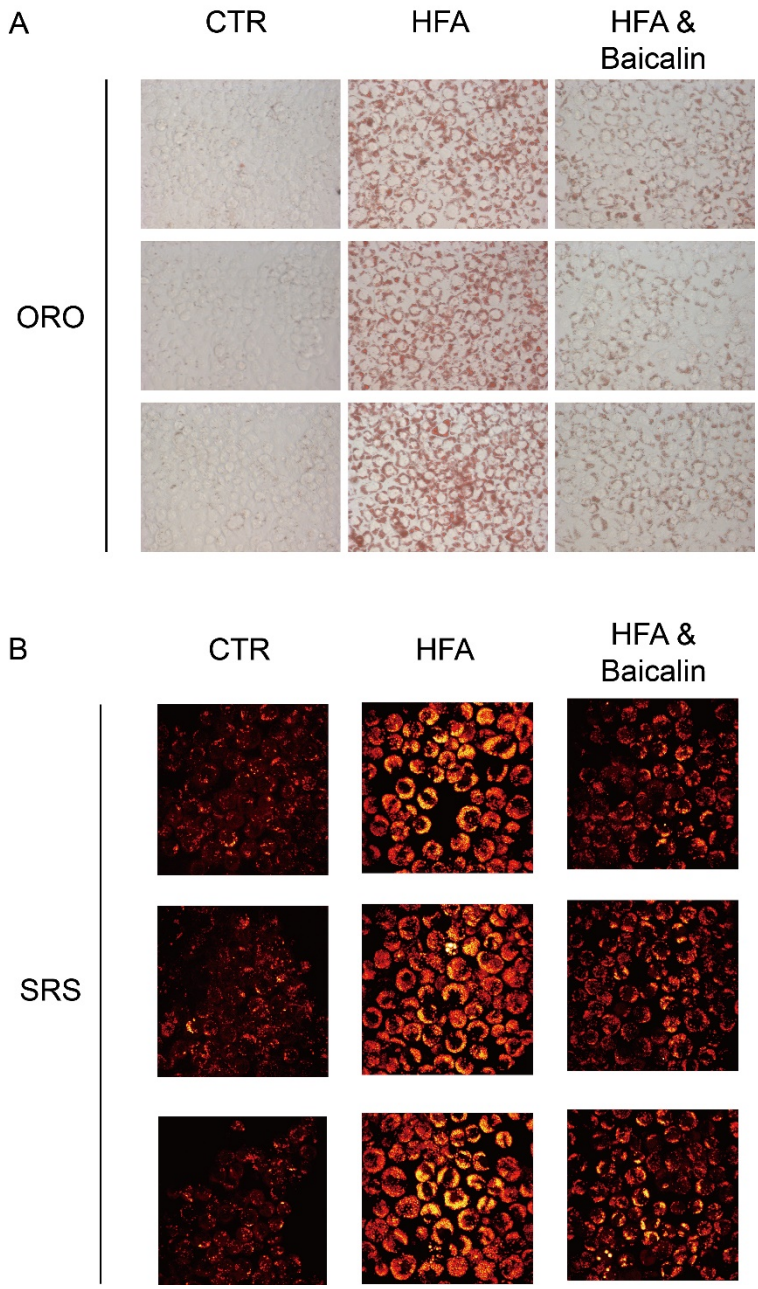

Fig. S1.

Baicalin reduces lipid accumulation in HeLa cells. **(A)** Images of Oil red O staining of HeLa cells treated with DMSO, high concentration of fatty acid or together with baicalin (100 μM baicalin for 24h, n=3) **(B)** Images of Stimulated Raman Scattering Microscopy analysis of lipid content in HeLa cells treated with DMSO, high concentration of fatty acid together with baicalin (100 μM baicalin for 24h, n=3).

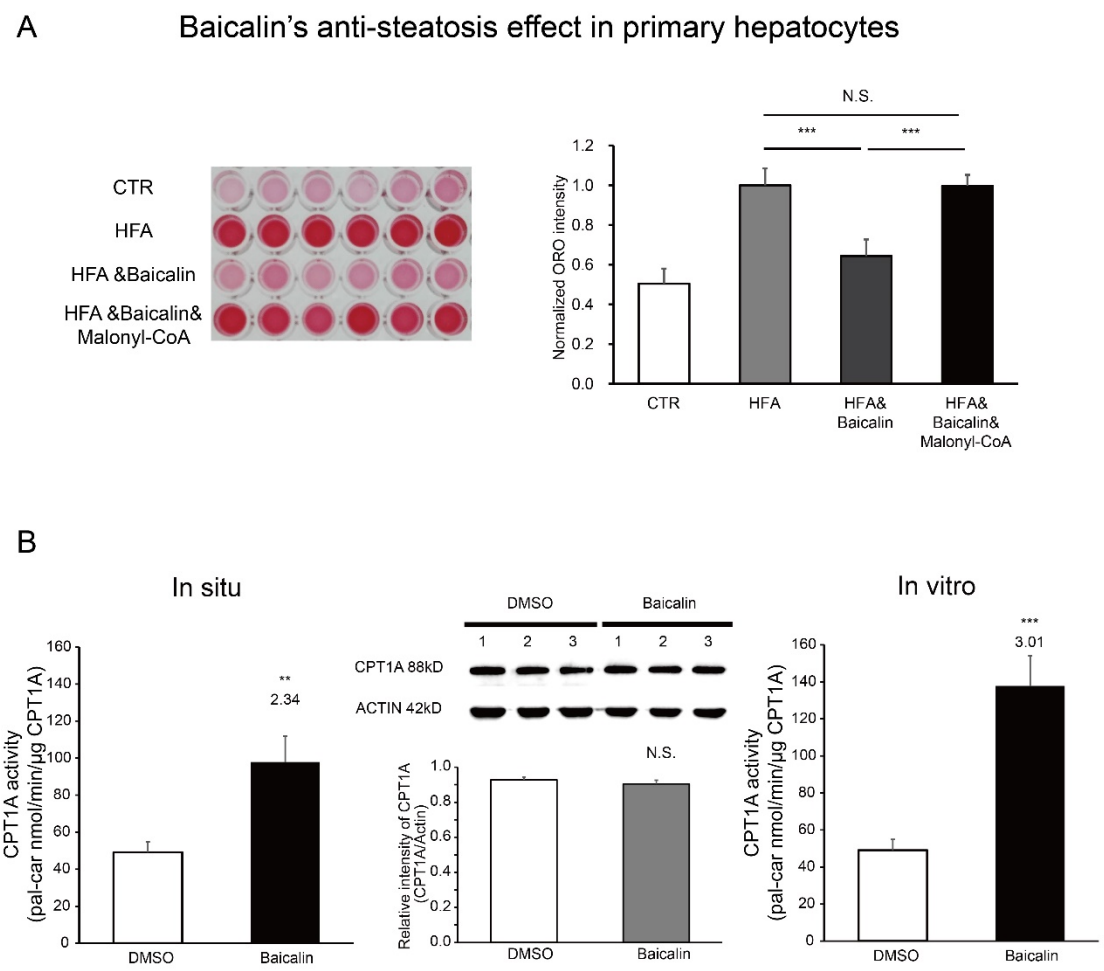

Fig. S2.

Baicalin reduces cellular lipid accumulation and directly activates CPT1A in primary hepatocytes isolated from mouse liver. **(A)**Images (left) and quantitation (right) of the extracted ORO dyes from the stained primary hepatocytes that were treated with DMSO ("CTR"), high concentration of fatty acids alone ("HFA") and together with baicalin and/or malonyl-CoA **(B)** (Left) Treatment of live hepatocytes with 100 μM of baicalin resulted in increased CPT1A activity. (Middle) Immunoblots of CPT1A and quantification of its protein abundance in hepatocytes with or without baicalin treatment. (Right) Treatment of hepatocyte lysates with 100 μM of baicalin resulted in increased CPT1A activity. Cells were assayed after treatment of 100 μM baicalin for 24h, n=6. * $p<0.05$; ** $p<0.01$; *** $p<0.001$

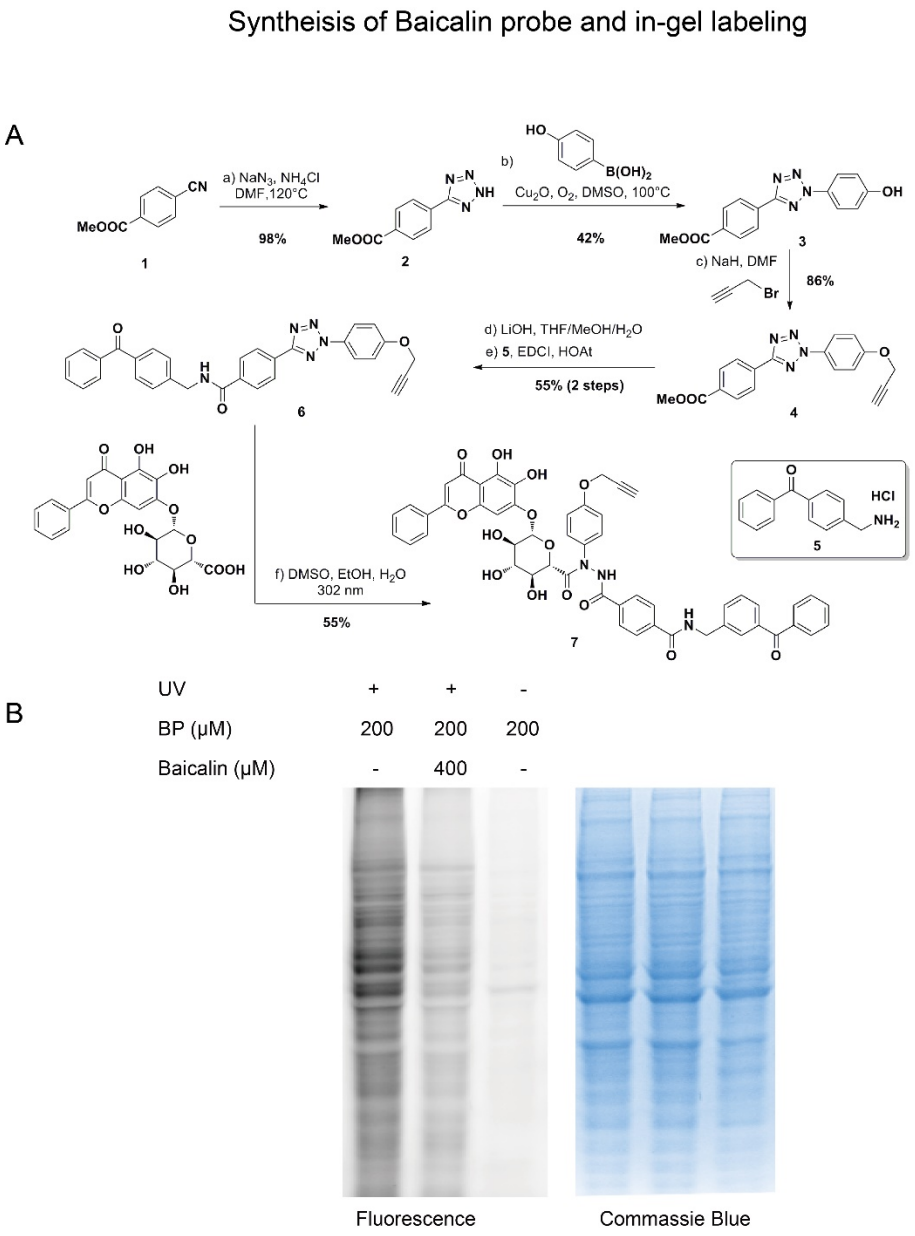

Fig. S3.

The synthetic route and in-gel fluorescence analysis of the baicalin photo-affinity probe. **(A)** Synthetic route. Reagents and conditions: a) NaN3 (1.5 equiv), NH4Cl (1.0 equiv), DMF, 120 °C, overnight, 98 %; b) (4-hydroxyphenyl)boronic acid (2.0 equiv), Cu2O (0.05 equiv), DMSO, 100 °C, overnight, 42 %; c) 3-bromoprop-1-yne (1.2 equiv), NaH (1.2 equiv), DMF, 0 to 25 °C, overnight, 86 %; d) LiOH·H2O (5.0 equiv), THF, MeOH, 65 °C, 2 h; e) (4-(aminomethyl)phenyl)(phenyl)methanone (1.1 equiv), EDCI (1.1 equiv), HOAT, (1.1 equiv), EA, 25 °C, 4 h, 55 % (2 steps); f) Baicalin (1.0 equiv), EtOH, H2O, DMSO, 302 nm UV, 25 °C, 3 h, 55 % (HPLC separation). **(B)** The HeLa cell proteomes were labeled with 200 μM of the baicalin probe and UV-dependent labeling signals were observed. In presence of 2-fold excess of baicalin, the labeling signals were effectively competed.

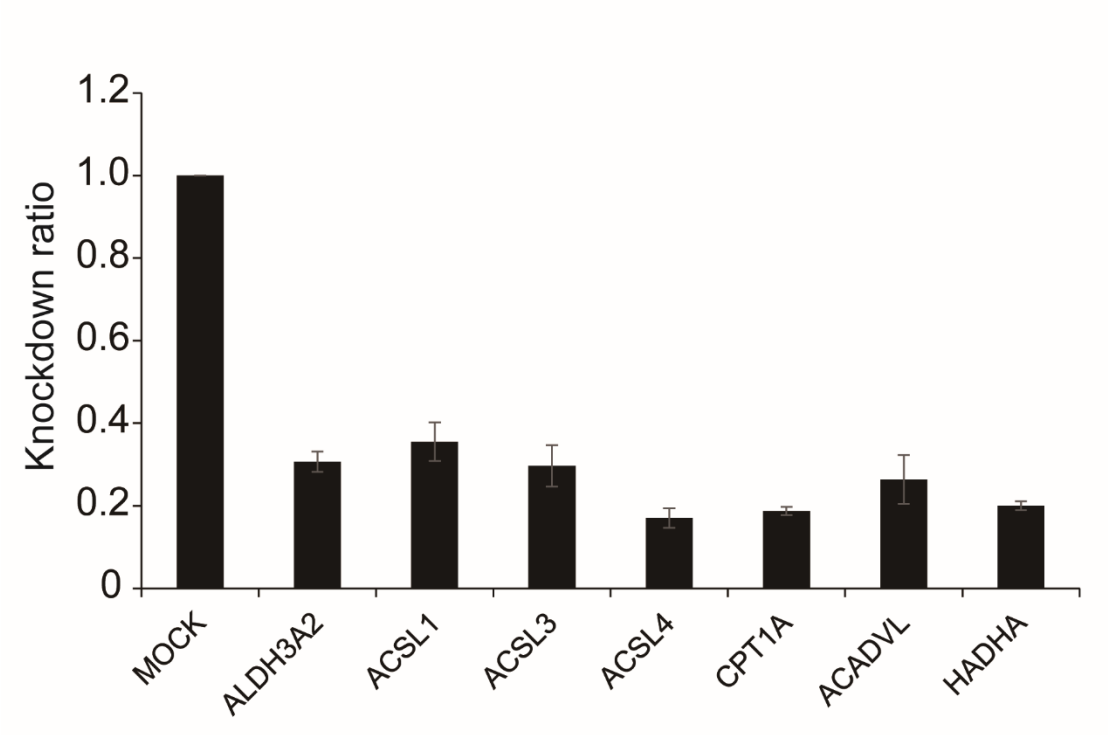

Fig. S4.

RNAi knockdown of seven enzymes in HeLa cells. The RT-PCR analysis shows that the mRNA levels of seven enzymes, which are identified as baicalin-binding targets and functionally assigned into the "fatty acid degradation" pathway as listed in Figure 2E, is reduced after RNAi knockdown. n=3

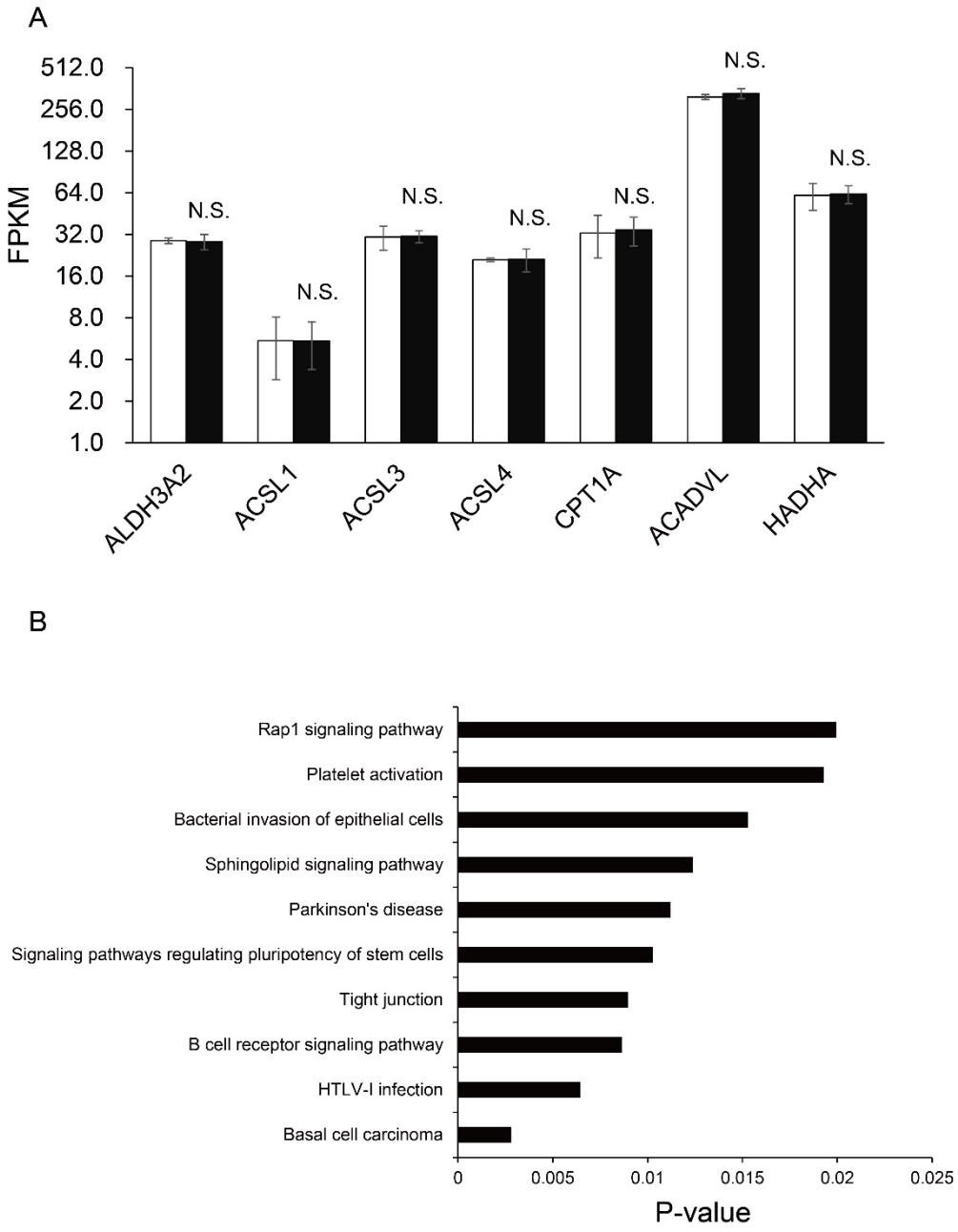

Fig. S5.

Baicalin does not affect lipid-metabolism related enzymes transcriptionally in HeLa cells as revealed by transcriptome analysis using RNA-seq. **(A)**FPKM values for the mRNAs of the seven enzymes that are identified as baicalin-binding targets and functionally assigned into the "fatty acid degradation" pathway as listed in Figure 2E. n=3. **(B)**The Gene Ontology analysis of the genes with significant changes at mRNA level after baicalin treatment ($p<0.05$) shows that pathways associated with lipid metabolism were not affected at the transcriptional level by the treatment of baicalin.

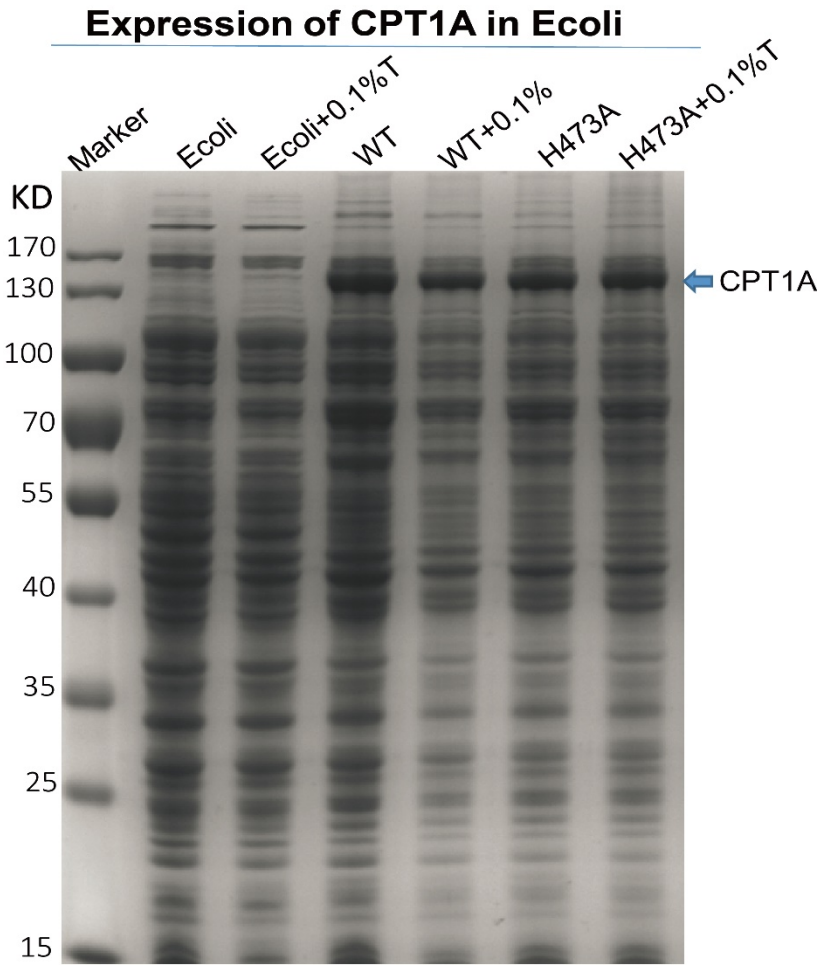

Fig. S6.

Recombinant expression of CPT1A in E.coli. SDS-PAGE of the E.coli lysates overexpressing RBP-CPT1A (WT or H473A) prepared with or without 0.1% Triton X-100 in the lysis buffer. The CPT1A was co-expressed with a maltose-binding protein (MBP) fused at the N-terminal separated by a TEV protease cleavable sequence. The predicted molecular weight of the final product is ~130kDa.

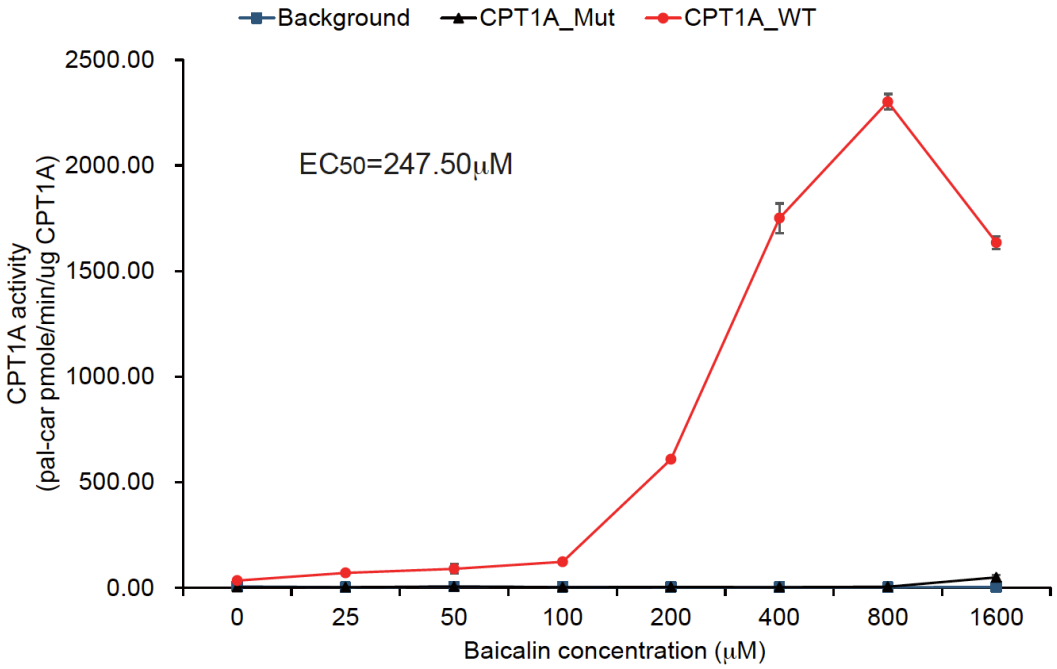

Fig. S7.

Baicalin showed a dose-dependent activation on recombinant CPT1A in E.coli lysates. CPT1A activity using E.coli lysates overexpressing an empty vector ("background") or a catalytically dead mutant H473A of CPT1A ("CPT1A_Mut") were included as controls. Assuming the activation effect reaches its maximum at 800 μM of baicalin, an estimated EC50 value can be fitted as 247.50 μM. n=3

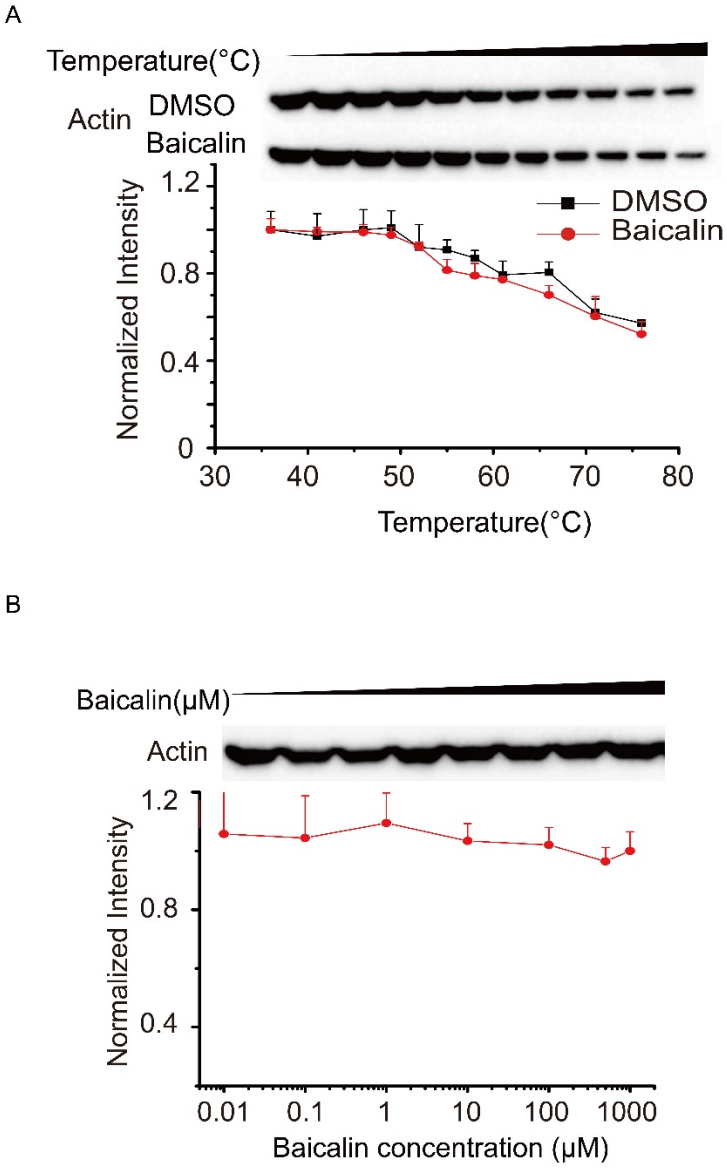

Fig. S8.

The thermal shift assay of a control protein, actin upon baicalin treatment-actin interaction. (A) Baicalin treatment (100 μM) didn't affect the thermal stability of CPT1A in cell lysates as measured by the temperature-dependent cellular thermal shift assay (n=3). (B) Baicalin treatment didn't affect the thermal stability of CPT1A in cell lysates as measured by the concentration-dependent cellular thermal shift assay at 52 °C (n=3).

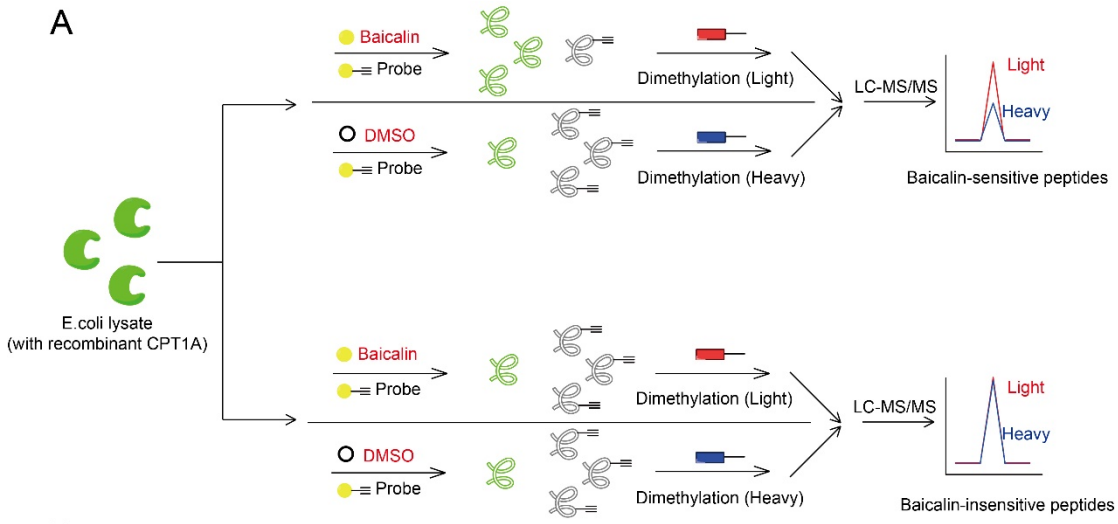

B

CPT1A_human

```
MAEAHQAV AFQFTVT PDGIDLRL SHEAL RQIYLSGLH SWK   40
KKFIRFKNG II TGVYPA SPSSWLI VVVGV MT TMYAK IDPS   80
LGII AK INRTLET AN CMSSQTKNV VSGVL FGTGLWV AL IV  120
TMRYSLKV LL SYHGWM FTEHGKMS RATK IWMGMV KI FSGR  160
KPML YSFQTSLPRL PVPAVK DTV NRYL QSVRPLMKE EDFK  200
RMTAL AQDFAV GLG PRLQWYLKLK SWWAT NYVSDWWEEYI  240
YL RGRGPLMV NSNYY AMD LL YILPTHI QAARAGNA IHAIL  280
LYRRKLD REEIKP IRLL GSTIPL CSAQWERMFNTSRIPGE  320
ETDT IQHMRDSKHI VVY HRGRYFK VWLYHDG RLLK PREME  360
QQMQRILDNTSEPQPGEARL AALT AGDRV PWA RCRQAYFG  400
RGKNKQ SLDAVEK AA FFVT LDETEEGYRSEDPDTSMDSYA  440
KSLL HGRCYD RWFDKSFTFVVFK NGKM GLNAEH SWADA PI  480
VAH LWEYVM SIDSLQL GYAEDGHCKGD INPNI PYPTRL QW  520
DI PGECQEV IETSLNTA NL LANDV DFHSFPFVAF GKG II K  560
KCRTSPDAFV QLALQL AHYK DMGKF CL TYEA SMTRL FREG  600
RTETVRSCTTE SCDFVRAMV DPAQTVEQRLKL FKLA SEKH  640
QHMY RLAMTGSGI DRHLF CLYV VSKYLA VE SPFLKEV LSE  680
PWRLSTSQT PQQQVEL FDLENN PEYV SSGGGFGPVADDGY  720
GVSY IL VGENL INFHISSK FSCPETDSHR FGRHLKEA MTD  760
II TL FGLSSNSKK  773
```

Fig. S9.

Identification of CPT1A peptides sensitive to the binding of baicalin by competitive ABPP-RD experiments. **(A)** Overall scheme of the competitive ABPP-RD experiments. Lysates of E.coli overexpressing CPT1A were first incubated with DMSO or baicalin separately and then labeled by the baicalin probe via UV photo-crosslinking. The probe labeled lysates were digested by trypsin and isotopically labeled by reductive dimethylation before being mixed together for LC-MS/MS analysis. Since baicalin could compete with the probe labeling and result in more unmodified peptides from CPT1A around the flavonoid's binding site, peptides with a higher quantification ratio (baicalin vs. DMSO) indicates their proximity to the binding site of baicalin whereas peptides on surface with unchanged ratios indicates their distance away from the binding site. **(B)**The amino acid sequence of CPT1A with the peptides with higher ratios colored in magenta and the peptides with unchanged ratios colored in purple.

A

	Stability (REU)	Binding (REU)
WT	0	0
L286W	-1.374	17.809
I291F	-0.843	7.888
E309Y	-2.56	3.871
H327E	-1.991	3.807

B

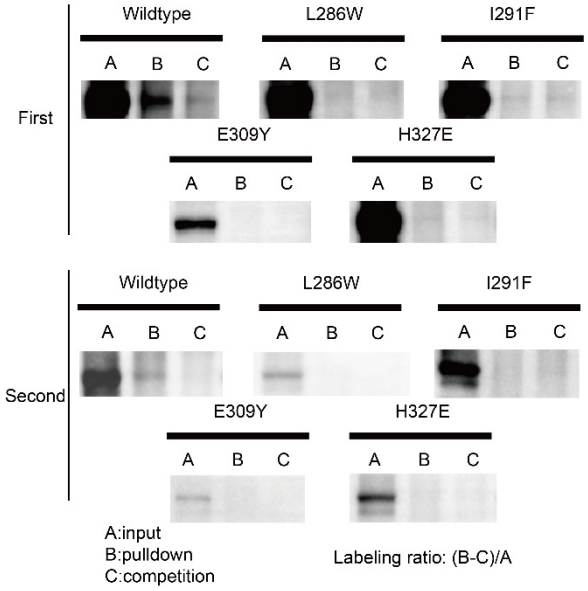

Fig. S10.

Evaluating the labeling of the baicalin probe on CPT1A mutants with disruptive mutations. (A) The list of Rosetta energy scores for the four "disruptive" mutants showing that they are predicted to maintain CPT1A stability (negative "stability" energy score) and to disrupt the binding with baicalin (positive "binding" energy score). **(B)** Disruptive mutations of predicted key interface residues abolished CPT1A labeling by the baicalin photo-affinity probe (n=2). Four disruptive mutations were predicted based the docking model of the CPT1A-baicalin complex. E.coli lysates overexpressing these mutants were labeled by the baicalin probe with or without baicalin competition and enriched by streptavidin. Immunoblotting analysis of CPT1A were performed for the input lysate before enrichment("input"), the sample after enrichment ("pulldown") and the sample after enrichment with baicalin competition ("competition"). The intensity of immunoblotting signals were quantified by ImageJ and a quantitative ratio of probe labeling (shown in Figure 4E) was calculated by subtracting the intensity from the "competition" lane from that of the "pulldown" lane, then divided by that of the "input" lane.

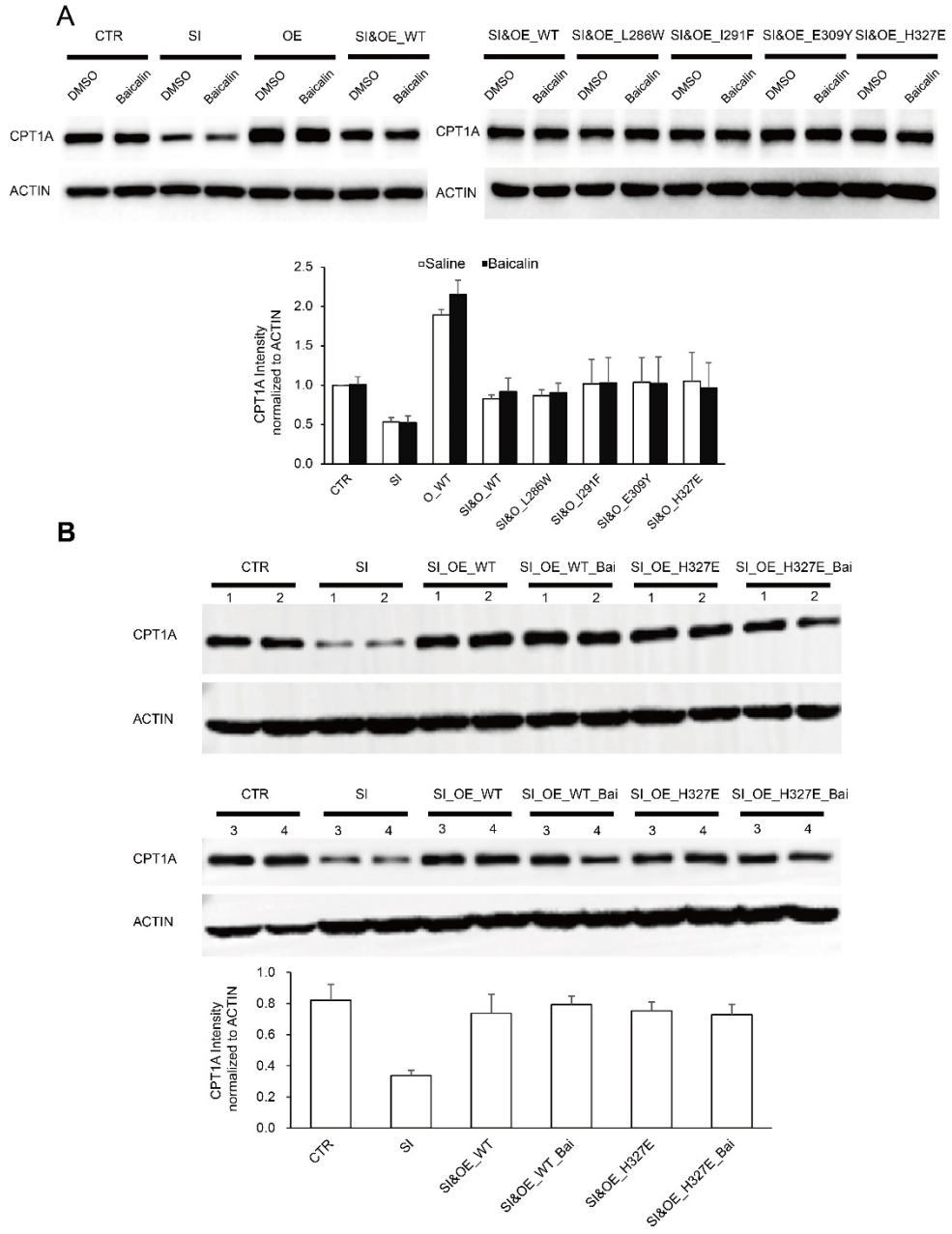

Fig. S11.

Abundance of CPT1A after endogenous knockdown and exogenous overexpression in the "rescuing" experiments. **(A)** Immunoblotting of CPT1A in HeLa cells after RNAi knockdown of endogenous CPT1A followed by transient overexpression of wild-type human CPT1A or baicalin-insensitive mutants. 100 μM baicalin for 24h, n=3. **(B)** Immunoblotting of CPT1A in mouse livers after shRNA knockdown of hepatic CPT1A followed by AAV-mediated overexpression of wild-type mouse CPT1A or its baicalin-insensitive H327E. CTR: control group, SI: Knockdown of endogenous CPT1A. OE: Overexpression of wild-type CPT1A or its baicalin-insensitive mutants. n=4

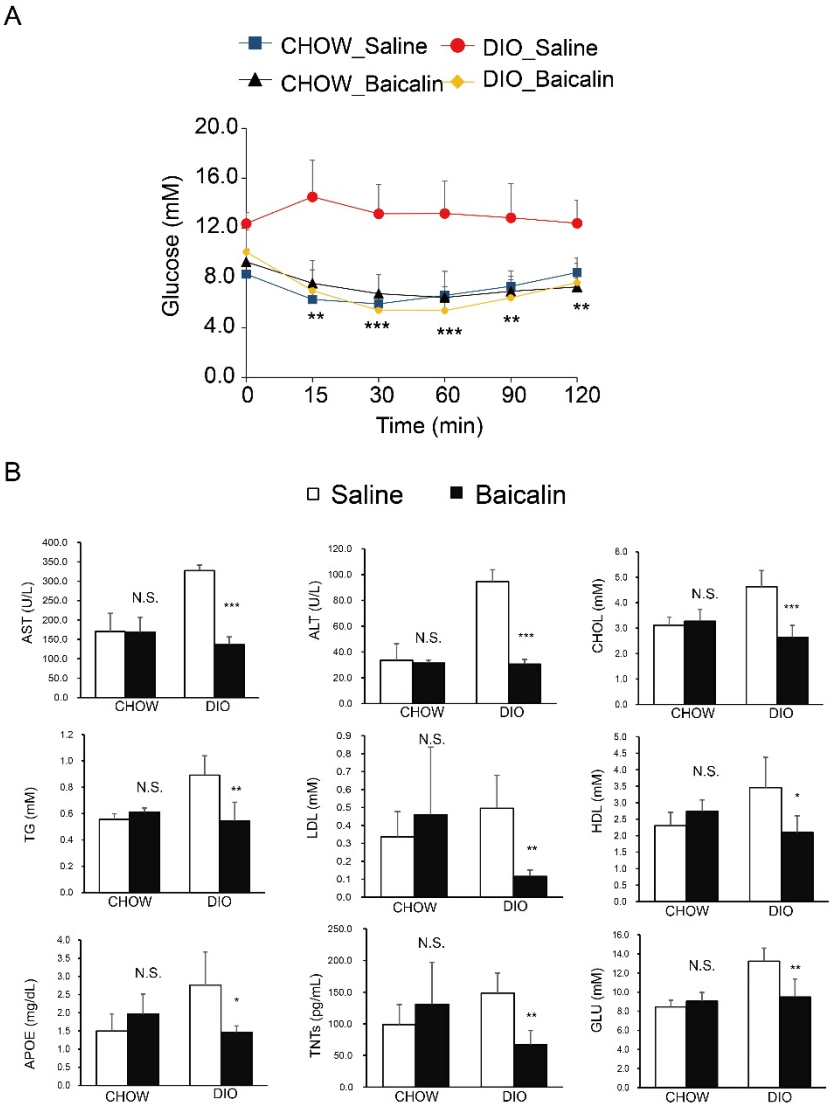

Fig. S12.

Baicalin treatment improves insulin sensitivity, hyperlipemia and hyperglycemia and liver functions. **(A)** Insulin Tolerance Test ("ITT") in chow and DIO mice. **(B)** Biochemical analysis of major biomarkers in blood of mice. The mice were on normal or high fat diet, and treated with or without baicalin. The biomarkers in blood were analyzed by corresponding kits including aspartate transaminase (AST), alanine transaminase (ALT), apolipoprotein E (APOE), cholesterol (CHOL), triglyceride (TG), glucose(GLU), high-density lipoprotein (HDL), low-density lipoprotein (LDL), troponin I and troponin T (TNTs). Baicalin reversed almost all of the disorders of NAFLD-related biochemical indexes. All data were measured after the daily treatment of saline or 400 mg/kg baicalin for 12 weeks,* $p<0.05$; ** $p<0.01$; *** $p<0.001$, n=5

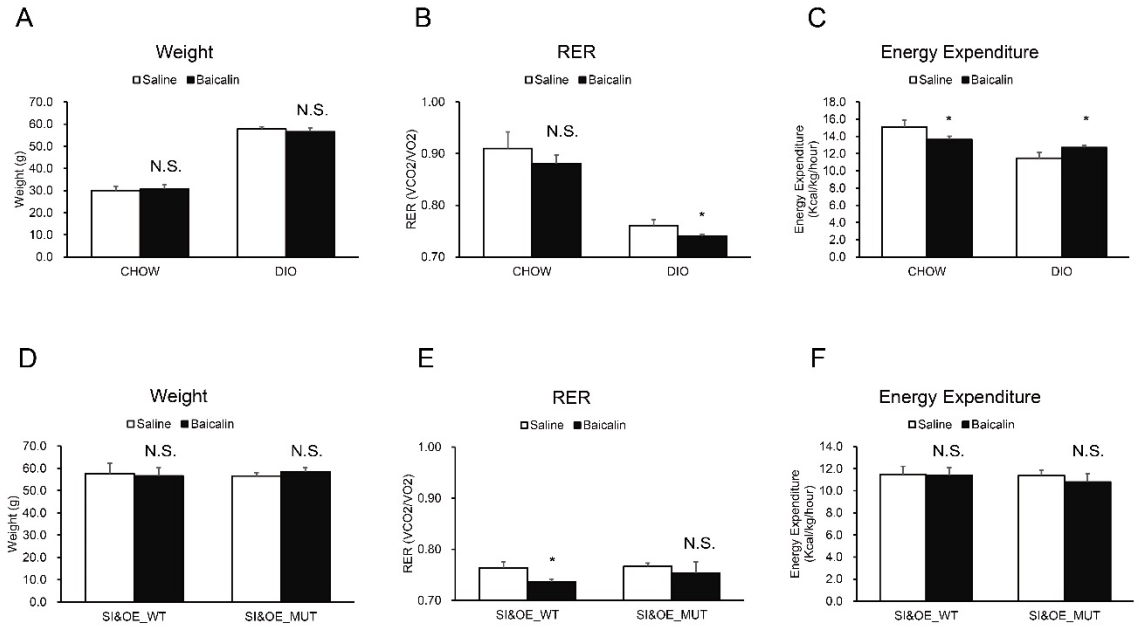

Fig. S13.

Baicalin treatment shifted the respiratory exchange ratio (RER) in DIO mice before body weights were diverged. (A) Baicalin treatment did not reduced the body weights in DIO mice or CHOW mice. (B) Baicalin treatment shifted the respiratory exchange ratio (RER) towards 0.7 in DIO mice, suggesting more fat is used as the energy source. (C) Baicalin treatment increased the energy expenditure in DIO mice and decreased the energy expenditure in CHOW mice. (D) Baicalin treatment did not reduced the body weights in DIO mice with overexpression of wild-type CPT1A (SI&OE_WT) or the disruptive mutant H327E (SI&OE_MUT) in mouse liver after knockdown of endogenous hepatic CPT1A (E) Baicalin treatment shifted the respiratory exchange ratio (RER) towards 0.7 in SI&OE_WT mice, suggesting more fat is used as the energy source. (F) Baicalin treatment didn't affect the energy expenditure significantly in SI&OE_WT or SI&OE_MUT mice at the third week. All data were measured after the daily treatment of saline or 400 mg/kg baicalin for 3 weeks,* $p<0.05$; ** $p<0.01$; *** $p<0.001$，n=5

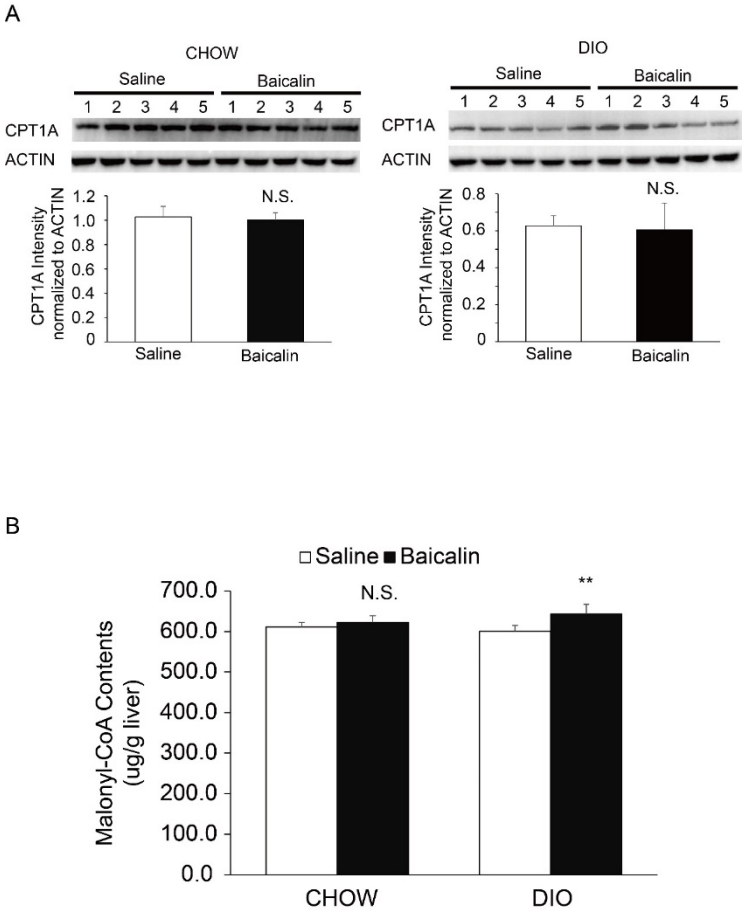

Fig. S14.

Baicalin treatment does not change expression of CPT1A and the level of malonyl-CoA in mouse livers. (**A)**Immunoblots of CPT1A and actin in livers of mice on normal and high-fat diet treated with or without baicalin, and the quantitation of levels of protein expression. **(B)** The level of Malonyl-CoA in livers of mice (on normal or high-fat diet) do not decreased significantly after treatment with baicalin. All data were measured after the daily treatment of saline or 400 mg/kg baicalin for 12 weeks, ** $p<0.01$; n=5.

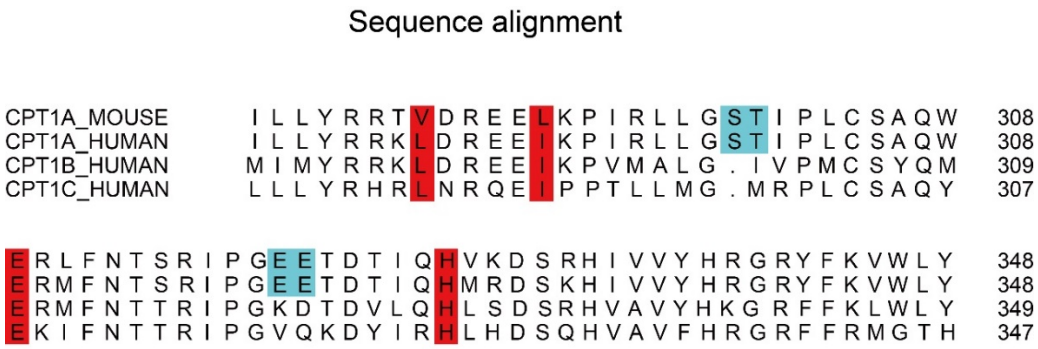

Fig. S15.

Selection of a baicalin-insensitive mutants in mouse CPT1A. Sequence alignment of human CPT1A, CPT1B, CPT1C and mouse CPT1A in the region of predicted binding site for baicalin. The residue positions for the four disruptive mutations predicted based on the docking model were highlighted in red. L286 and I291 are not conserved between human and mouse CPT1A orthologues. The regions that are conserved between human and mouse orthologues but between human CPT1A isoforms are highlighted in cyan, which could be responsible for the isoform selectivity of baicalin on human CPT1A.

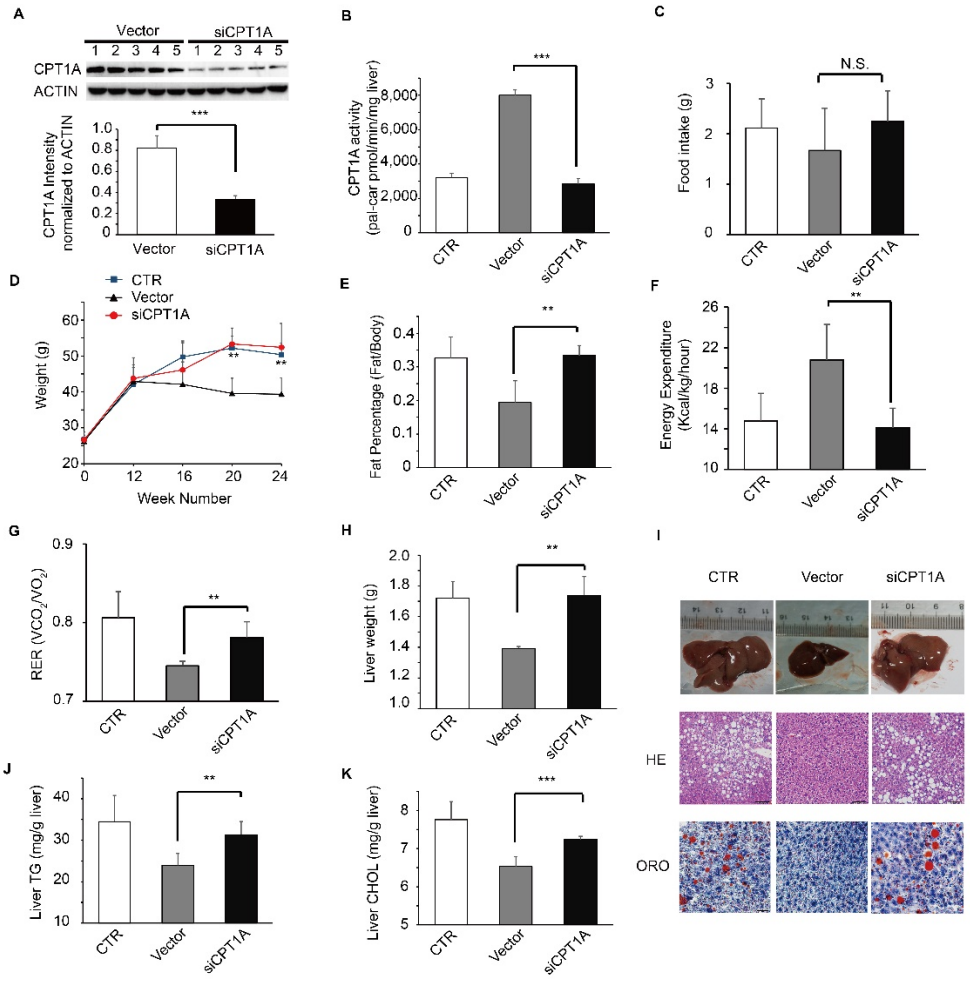

Fig. S16.

Knockdown of hepatic CPT1A abolished the anti-steatosis effect of baicalin in DIO mice. (A) Immunoblots (top) and quantitation (bottom) of hepatic CPT1A after the tissue-specific knockdown by shRNA interference (siCPT1A). (B) Knockdown of hepatic CPT1A resulted in decreased the enzyme activity of CPT1A in mouse liver. (C) Knockdown of hepatic CPT1A does not affect food intake in DIO mice. (D) Knockdown of hepatic CPT1A abolished the reduction of body weight induced by baicalin in DIO mice. (E) Knockdown of hepatic CPT1A abolished the reduced percentage of body fat induced by baicalin in DIO mice. (F-G) Knockdown of hepatic CPT1A abolished the increased the energy expenditure and the shifted respiratory exchange ratio (RER) induced by baicalin in DIO mice. (H) Knockdown of hepatic CPT1A abolished the reduced liver weights induced by baicalin in DIO mice. (I) Knockdown of hepatic CPT1A abolished the reduced liver sizes and hepatic steatosis induced by baicalin in DIO as measured by HE and ORO staining. (J-K) Knockdown of hepatic CPT1A abolished the reduced levels of hepatic triglyceride (TG) and cholesterol (CHOL) induced by baicalin in DIO mice. All data were measured after the daily treatment of saline or 400 mg/kg baicalin for 12 weeks, * $p<0.05$; ** $p<0.01$; *** $p<0.001$, n=5.

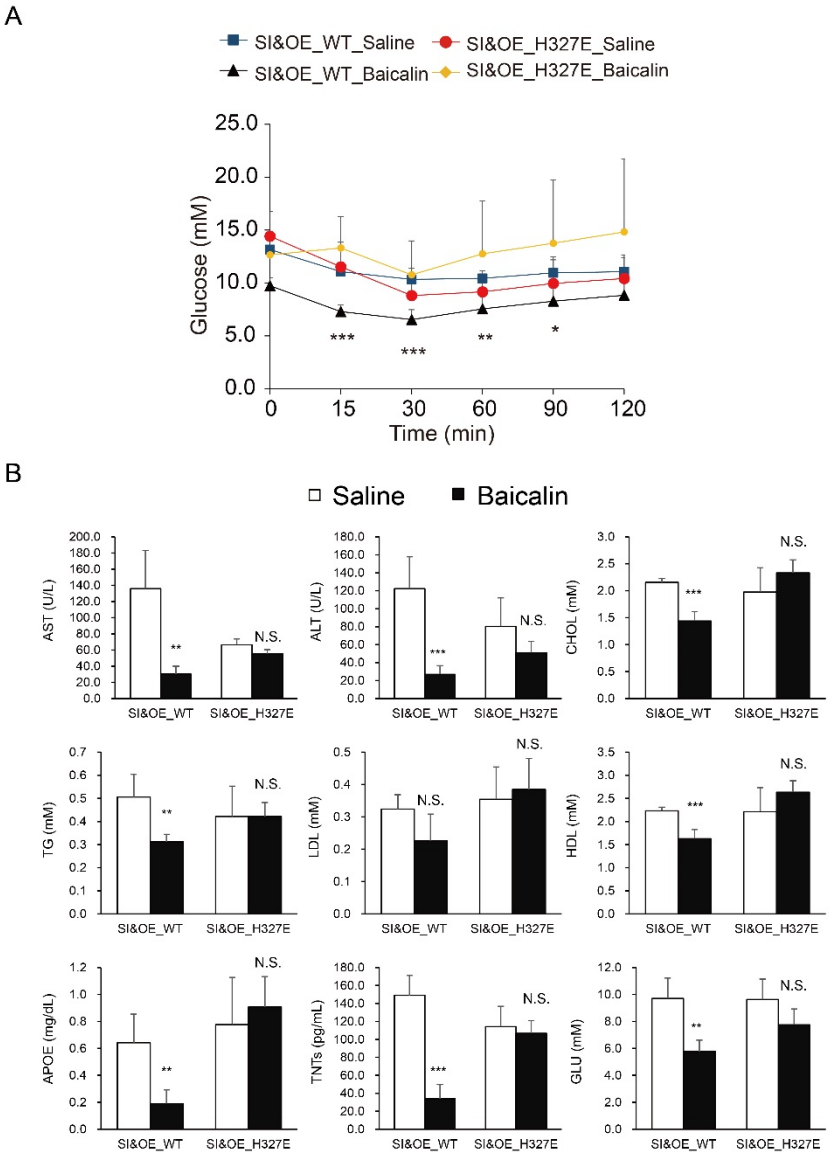

Fig. S17.

Systemic improvement of insulin resistance and other metabolic parameters by baicalin is dependent on its interaction with CPT1A. **(A)** Insulin Tolerance Test ("ITT") in DIO mice with overexpression of the wildtype CPT1A and H327E mutant. **(B)** Biochemical analysis of major biomarkers in blood of mice. The mice were on normal or high fat diet, and treated with or without baicalin. The biomarkers in blood were analyzed by corresponding kits including aspartate transaminase (AST), alanine transaminase (ALT), apolipoprotein E (APOE), cholesterol (CHOL), triglyceride (TG), glucose(GLU), high-density lipoprotein (HDL), low-density lipoprotein (LDL), troponin I and troponin T (TNTs). Baicalin reversed almost all of the disorders of NAFLD-related biochemical indexes. All data were measured after the daily treatment of saline or 400 mg/kg baicalin for 12 weeks,* $p<0.05$; ** $p<0.01$; *** $p<0.001$，n=5

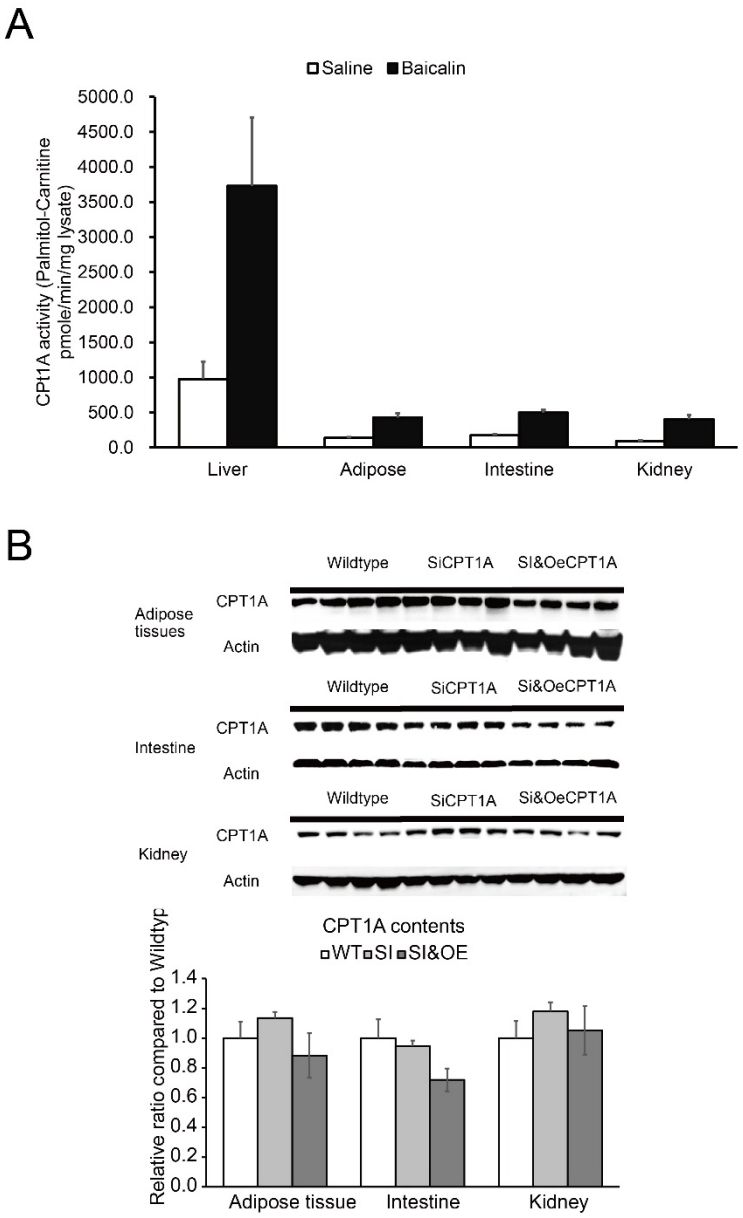

Fig. S18.

The abundance and activity of CPT1A in other tissues such as adipose, intestine and kidney. (A) CPT1A could be activated by baicalin across all these tissues with the overall activity of hepatic CPT1A measured as the highest one. All data were measured after the daily treatment of saline or 400 mg/kg baicalin for 12 weeks, n=4. (B) Western blotting of CPT1A in three additional tissues including adipose, intestine and kidney from control mice, mice with CPT1A knockdown as well as mice with CPT1A restoration. n=4

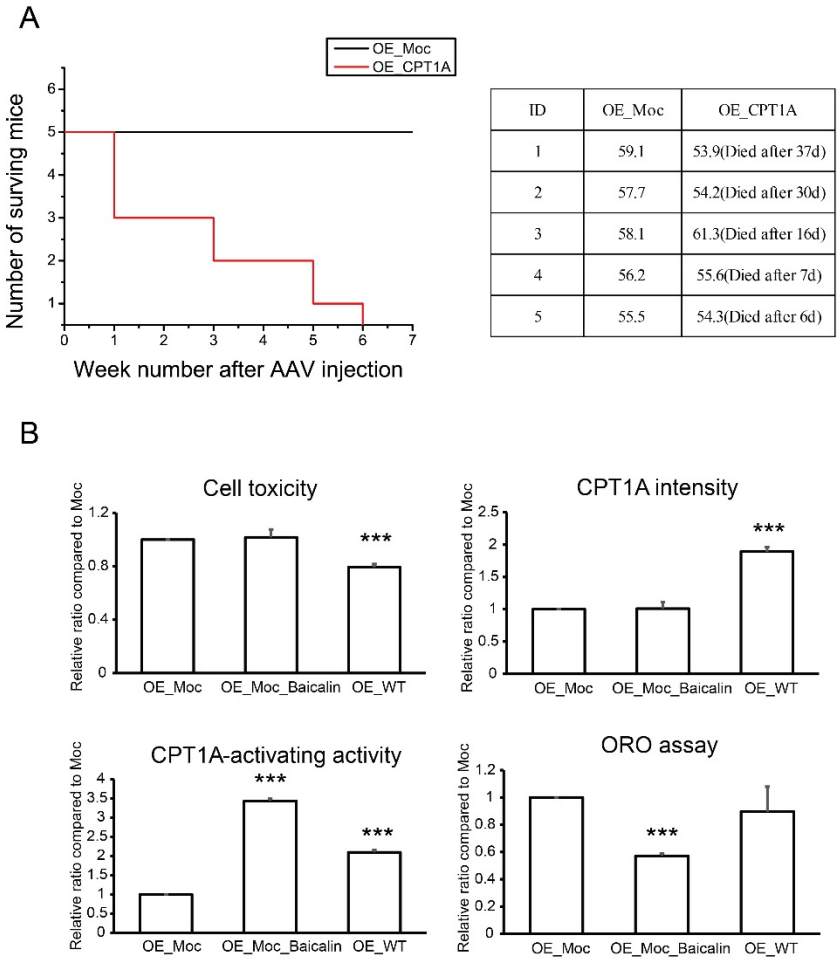

ID	OE_Moc	OE_CPT1A
1	59.1	53.9(Died after 37d)
2	57.7	54.2(Died after 30d)
3	58.1	61.3(Died after 16d)
4	56.2	55.6(Died after 7d)
5	55.5	54.3(Died after 6d)

Fig. S19.

Overexpression experiments of CPT1A in DIO mice and HeLa cells. (A) Overexpressing CPT1A by an adeno-associated virus with a strong liver-specific promoter resulted in premature death of mice (B) Evaluation of the cell toxicity, CPT1A abundance, CPT1A-activating ability and lipid-reducing effects of transient CPT1A overexpression and baicalin treatment in HeLa cells.(100 μM baicalin for 24h, n=3) * $p<0.05$; ** $p<0.01$; *** $p<0.001$

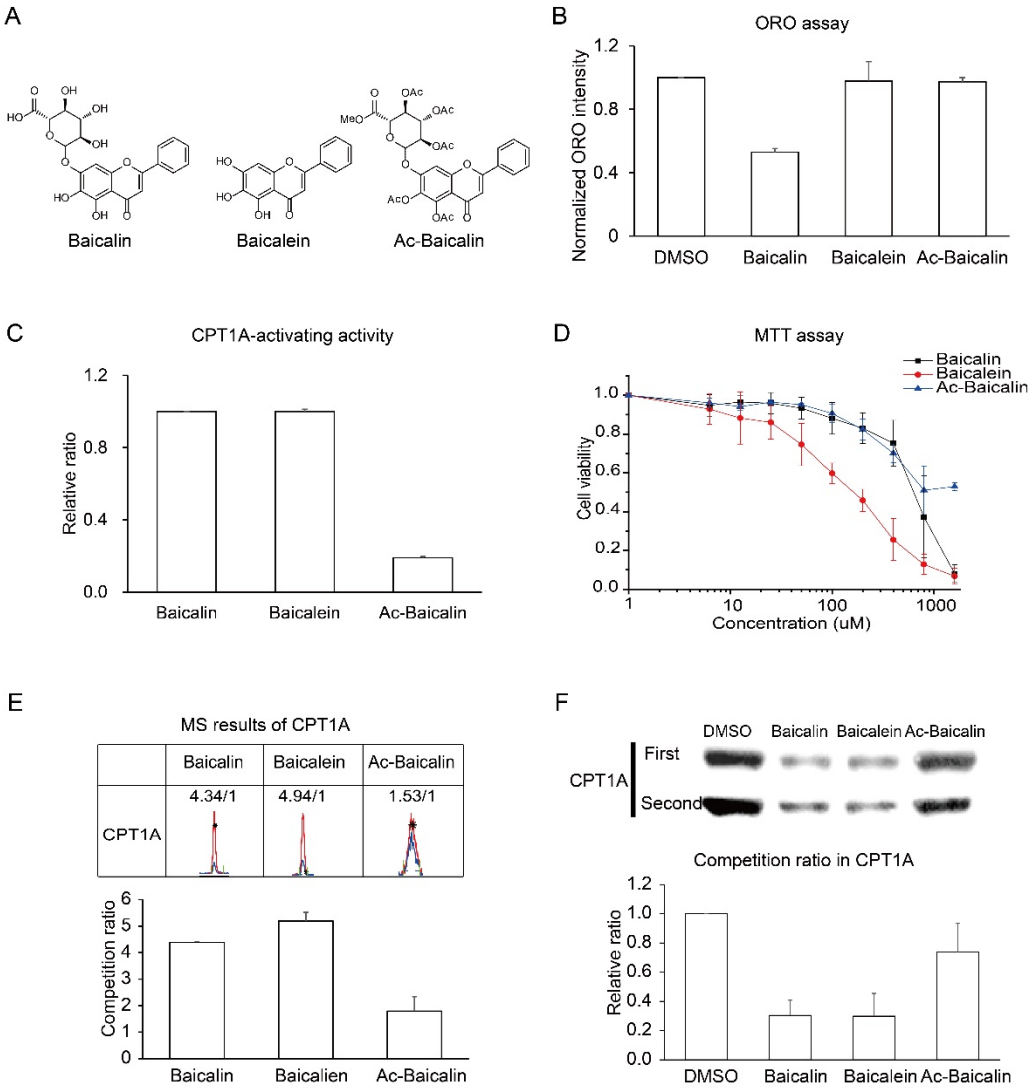

Fig. S20.

Evaluation of baicalin derivatives in activing CPT1A and reducing lipid accumulation. (A) Structure of baicalin, baicalein and Ac-baicalin (B) Evaluation of the lipid-reducing effects of baicalin, baicalein and Ac-baicalin in HeLa cells using the Oil red O (ORO) staining (100 μM baicalin derivatives for 24h, n=3). (C) Comparison of the CPT1A-activating ability of baicalin, baicalein and Ac-baicalin using crude lysates from E.coli overexpressing wild-type CPT1A. (n=3) (D) Evaluation of the cytotoxicity effects of baicalin, baicalein and Ac-baicalin in HeLa cells using the MTT assay (100 μM baicalin derivatives for 24h, n=3). (E) Competition to the photo-labeling of the baicalin-probe on CPT1A by baicalein and Ac-baicalin as demonstrated by chemical proteomic profiling experiments (top: raw chromatographic traces; bottom: averaged competition ratio). (E) Competition to the photo-labeling of the baicalin-probe on CPT1A by baicalein and Ac-baicalin as demonstrated by immunoblotting.

Dataset S1.
The list of all quantified protein in SILAC-ABPP experiments. The list contains SILAC ratios (light vs heavy) for proteins with quantified ratios from all the three replicates from each of the "BP-control", "CP-control", "UV-control" and "Competition" SILAC-ABPP experiments. The averaged ratios are shown in the last column.

Dataset S2.
The list of specific baicalin-binding proteins identified by SILAC-ABPP experiments. The data in Dataset S1 was filtered with an average ratio cutoff of 4.0 from each of the "BP-control", "CP-control", "UV-control" and "Competition" SILAC-ABPP experiments. There are 142 proteins that passes the criterion and they were used for further GO analysis. The seven proteins highlighted in red are from the functional cluster of "fatty acid degradation" as shown in Fig. 2E.

Dataset S3.
The transcriptome analysis of HeLa cells treated with DMSO and baicalin by RNA-seq. The "Raw Data" tab contains FPKM values for the mRNAs from a total of 22505 genes in triplicates. The "Selected Targets" tab contains FPKM values for each of the seven baicalin-binding proteins associated with "Fatty acid degradation" (as listed in Fig. 2E). The "GO analysis" tab contains the Gene Ontology analysis of the genes with significant changes at mRNA level after baicalin treatment ($p<0.05$, 827 genes in total) and it shows that pathways associated with lipid metabolism were not affected at the transcriptional level by the treatment of baicalin.

References

1. Gomez-Lechon MJ*, et al.* (2007) A human hepatocellular in vitro model to investigate steatosis. *Chemico-biological interactions* 165(2):106-116.
2. Yu Z*, et al.* (2012) Label-free chemical imaging in vivo: three-dimensional non-invasive microscopic observation of amphioxus notochord through stimulated Raman scattering (SRS). *Chemical Science* 3(8):2646.
3. Wanders RJ, Ruiter JP, L IJ, Waterham HR, & Houten SM (2010) The enzymology of mitochondrial fatty acid beta-oxidation and its application to follow-up analysis of positive neonatal screening results. *Journal of inherited metabolic disease* 33(5):479-494.
4. Martin BR, Wang C, Adibekian A, Tully SE, & Cravatt BF (2011) Global profiling of dynamic protein palmitoylation. *Nature methods* 9(1):84-89.
5. Weerapana E, Speers AE, & Cravatt BF (2007) Tandem orthogonal proteolysis-activity-based protein profiling (TOP-ABPP)--a general method for mapping sites of probe modification in proteomes. *Nature protocols* 2(6):1414-1425.
6. Boersema PJ, Raijmakers R, Lemeer S, Mohammed S, & Heck AJ (2009) Multiplex peptide stable isotope dimethyl labeling for quantitative proteomics. *Nature protocols* 4(4):484-494.
7. Xu T*, et al.* (2015) ProLuCID: An improved SEQUEST-like algorithm with enhanced sensitivity and specificity. *Journal of proteomics* 129:16-24.
8. Tabb DL, McDonald WH, & Yates JR, 3rd (2002) DTASelect and Contrast: tools for assembling and comparing protein identifications from shotgun proteomics. *J Proteome Res* 1(1):21-26.

9. Benjamin DI, Cravatt BF, & Nomura DK (2012) Global profiling strategies for mapping dysregulated metabolic pathways in cancer. *Cell metabolism* 16(5):565-577.
10. Zheng L, Baumann U, & Reymond JL (2004) An efficient one-step site-directed and site-saturation mutagenesis protocol. *Nucleic acids research* 32(14):e115.
11. Liu J, Lee J, Salazar Hernandez MA, Mazitschek R, & Ozcan U (2015) Treatment of obesity with celastrol. *Cell* 161(5):999-1011.
12. Xi Y*, et al.* (2015) Baicalin Attenuates High Fat Diet-Induced Obesity and Liver Dysfunction: Dose-Response and Potential Role of CaMKKbeta/AMPK/ACC Pathway. *Cell. Physiol. Biochem.* 35(6):2349-2359.
13. Rubinson DA*, et al.* (2003) A lentivirus-based system to functionally silence genes in primary mammalian cells, stem cells and transgenic mice by RNA interference. *Nat Genet* 33(3):401-406.
14. Yu JH*, et al.* (2016) Suppression of PPARgamma-mediated monoacylglycerol O-acyltransferase 1 expression ameliorates alcoholic hepatic steatosis. *Scientific reports* 6:29352.
15. Song R*, et al.* (2013) Central role of E3 ubiquitin ligase MG53 in insulin resistance and metabolic disorders. *Nature* 494(7437):375-379.
16. Kim DE, Chivian D, & Baker D (2004) Protein structure prediction and analysis using the Robetta server. *Nucleic acids research* 32(Web Server issue):W526-531.
17. Le Guilloux V, Schmidtke P, & Tuffery P (2009) Fpocket: an open source platform for ligand pocket detection. *BMC bioinformatics* 10:168.
18. Trott O & Olson AJ (2010) AutoDock Vina: improving the speed and accuracy of docking with a new scoring function, efficient optimization, and multithreading. *Journal of computational chemistry* 31(2):455-461.
19. Lemmon G & Meiler J (2012) Rosetta Ligand docking with flexible XML protocols. *Methods in molecular biology* 819:143-155.
20. Park H*, et al.* (2016) Simultaneous optimization of biomolecular energy function on features from small molecules and macromolecules. *Journal of chemical theory and computation*.
21. Savitski MM*, et al.* (2014) Tracking cancer drugs in living cells by thermal profiling of the proteome. *Science* 346(6205):1255784.
22. Martinez Molina D*, et al.* (2013) SI-Monitoring drug target engagement in cells and tissues using the cellular thermal shift assay. *Science* 341(6141):84-87.